Chapter 4

Plasma Enhanced Chemical Vapour Deposited Hydrogenated Silicon Films Using Layer-by-layer And Continuous Deposition Techniques

4.1 Introduction

This chapter will present the results obtained from the optical and structural characterization of hydrogenated silicon (Si:H) thin films deposited on crystal silicon (c-Si) and glass substrates by plasma enhanced chemical vapour deposition (PECVD) using layer-by-layer (LBL) and continuous deposition (CD) deposition techniques. The optical constants such as film thickness, refractive index and optical energy gap were determined from the optical transmission spectra of the films deposited on glass substrates measured using ultra-violet visible near-infrared (UV-VIS-NIR) spectroscopy technique. Fourier transform infrared (FTIR) spectroscopy and X-ray diffraction (XRD) were used to investigate the structural properties of the films. The FTIR transmission spectra were carried out to study the silicon-bonding configurations present in the films. The XRD characterization technique was used to observe evidence of crystallinity in the films. FTIR spectroscopy measurements were done on the films deposited on c-Si substrates only while XRD patterns were obtained from films deposited on both glass and c-Si substrates. The effects of rf power, substrate temperature and hydrogen to silane flow-rate ratio on the optical and structural properties of the films deposited by LBL and CD techniques are analyzed and compared. The properties of the films deposited by these techniques on glass and c-Si substrates are also studied and compared if the measurements can be done on both types of substrates. The objectives of this part of the work are, first to understand the deposition mechanism of the Si:H films grown by LBL deposition technique by comparing the influence of rf power, substrate temperature and hydrogen to silane flow-rate ratio on the growth rates of the LBL and CD films with respect to these parameters, second to compare the effect of the deposition parameters on the optical properties, the hydrogen incorporation into the film structure and the structural order of the films, and third to show that LBL deposited

films are more crystalline compared to CD films irrespective of the deposition parameters and these films are more crystalline on c-Si substrates.

4.2 Optical Transmission Spectra

The optical transmission spectra of the LBL and CD films were obtained using a UV-Vis-Nir spectrophotometer, model of Jasco V-570 for films deposited on glass substrates. The scanning range for this measurement was fixed at 190 to 2500 nm. The thickness, refractive index, absorption coefficient and optical energy gap of the films were obtained from the optical transmission spectra of the films. The effects of rf power, T_s and R on these parameters are presented and discussed in the following sections of this chapter.

Figure 4.1 shows typical optical transmission spectra of multiphase structured and a homogenous structured of Si:H thin films respectively. The corresponding XRD spectra of the films are shown next to the optical transmission spectra. The multiphase structured of Si:H thin film usually consists of Si nano-crystallites embedded in an amorphous Si matrix. The optical transmission spectrum of the homogeneous structured of amorphous Si:H film produced a group of interference pattern where the maximum and minimum points of the fringes could be joined by a continuous curve as shown in Figure 4.1(a). The maximum and minimum points of the spectrum produced by the multiphase structured film could not be joined by a single continuous line as shown in Figure 4.1(b). These spectra will be used to analyse the phase structure of the films represented by the optical transmission spectra of the films as shown in Figure 4.2.

Figure 4.2(a) and (b) suggested that both the LBL and CD films prepared on glass substrates at all rf powers were typically homogeneous structured of amorphous Si:H thin films which is in single phase structure. T_s showed significant influence on the phase structure of the LBL films. Increase in T_s showed increase in the number of

groups of interference fringes where the maximum and minimum points cannot be joined by a single continuous curve. These features were not observed in the optical transmission spectra of the CD films prepared at different T_s in Figure 4.2(d). R appeared to change the phase structures in the LBL film. Multiphase structured was observed in the film prepared at the lowest R of the CD films as indicated by the optical transmission spectrum of the film.

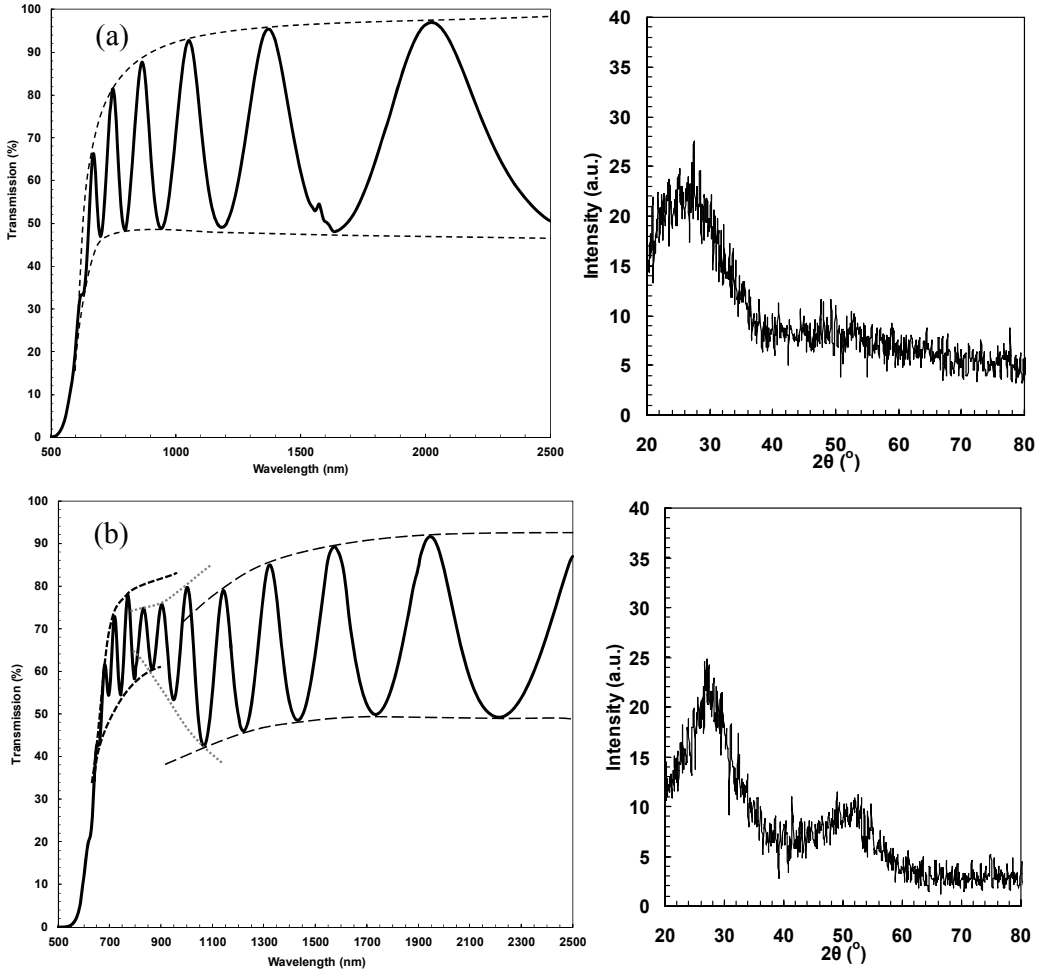

Figure 4.1: Typical optical transmission spectra with corresponding XRD spectra of (a) a homogenous structured of amorphous Si:H thin film and (b) multiphase structured of Si:H thin film.

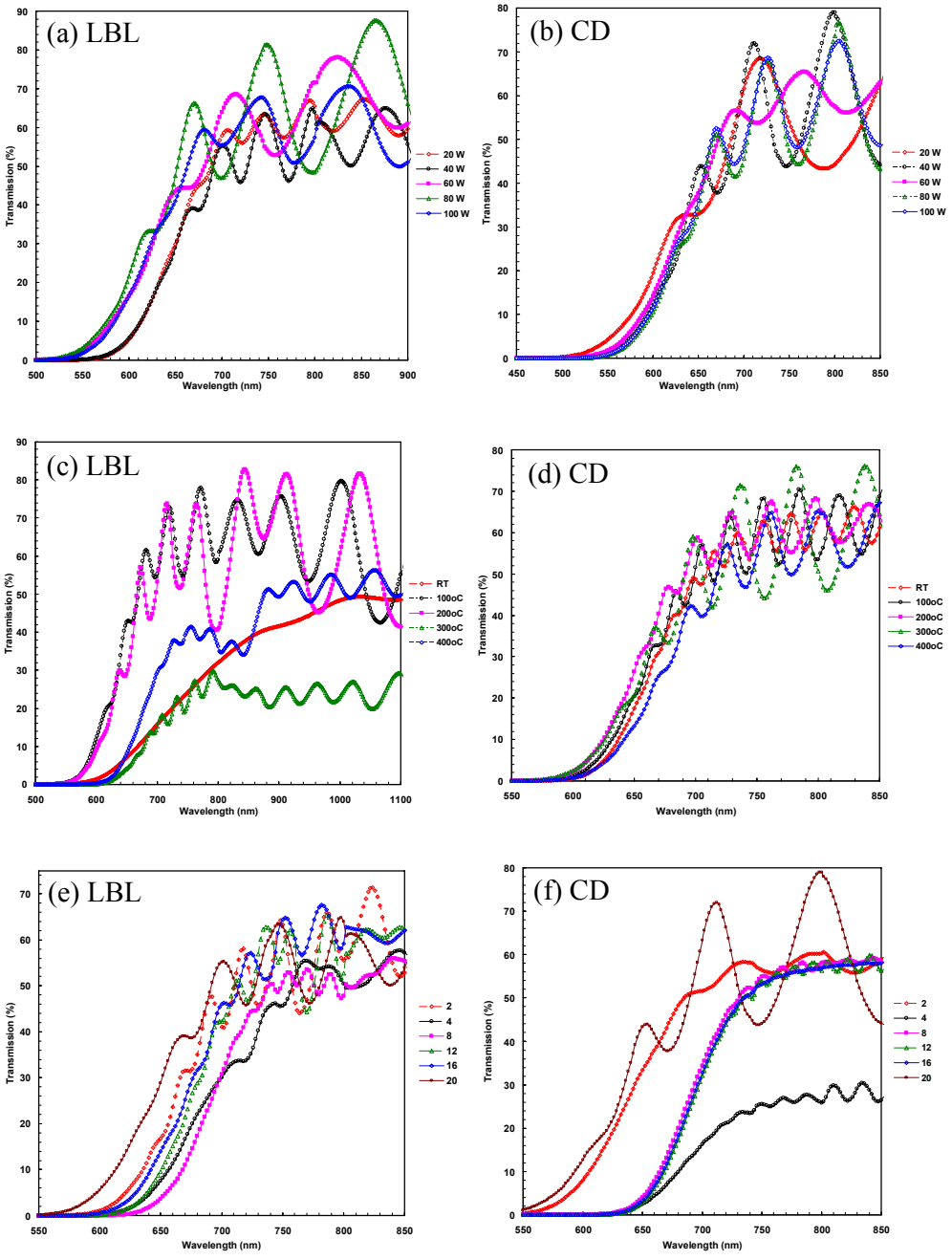

Figure 4.2: Optical transmission spectra for the LBL and CD films deposited at different rf powers (a) and (b), substrate temperatures, T_s (c) and (d) and hydrogen to silane flow-rate ratios, R (e) and (f) respectively.

4.2.1 Deposition Rate

In this work, the deposition rates of the films were determined from the film thickness divided by deposition time. Thicknesses of these films were estimated from interference fringes of optical transmission spectra using Manifacier and Davies techniques combined as described in Section 3.3.1.1. Table 4.1 tabulates the fixed and variable deposition parameters, and thicknesses of the Si:H thin films deposited by LBL and CD deposition techniques at different rf powers, T_s and R. Figure 4.3 shows the variation of deposition rate of the Si:H films grown by LBL and CD deposition techniques with rf power, T_s and R respectively. Figure 4.3(a) showed that deposition rate of the LBL films decreased from 7.7 to 3.4 Å/s as the applied rf power was increased from 20 to 60 W. The deposition rate remained unchanged with further increase in rf power to 100 W.

Table 4.1: Deposition parameters and thicknesses of Si:H films deposited by LBL and CD deposition techniques at different rf powers, substrate temperatures, T_s and hydrogen to silane flow-rate ratios, R.

Deposition parameters		Thickness (±108 nm)	
Fixed parameter	Variable parameter	CD	LBL
T_s & R	20 W	311.0	1385.5
	40 W	677.3	1136.2
	60 W	727.9	613.1
	80 W	714.5	667.3
	100 W	722.7	746.3
R & rf power	RT	3039.1	712.2
	100°C	2418.4	1151.1
	200°C	2020.3	1098.9
	300°C	1170.3	1635.6
	400°C	1493.9	2388.8
rf power & T_s	2	891.9	1793.9
	4	2838.4	2241.6
	8	4561.2	4029.1
	12	4946.7	2320.3
	16	7283.1	1878.5
	20	1262.5	1635.6

The CD films which were deposited using the same deposition conditions as the LBL films prepared at different rf powers showed a reversed trend in the variation of the deposition rate with respect to rf power. The deposition rate of the CD films increased slowly from 3.1 to 4 Å/s with increase in rf power from 20 to 60 W followed by no further increase in deposition rate with increase in rf power to 100 W.

High deposition rate of Si:H films prepared by rf PECVD are usually reported for films deposited at high rf power and high pressure (Das and Ray, 2002; Feitknecht *et al.*, 2001; Kondo *et al.*, 2000). In this work, the Si:H films deposited at low rf power of 20 W using LBL deposition technique was grown at a respectively high deposition rate of 7.7 Å/s. The increase in deposition rate with increase in rf power as shown by the CD films has also been reported by other researchers (Lebib and Cabarrocas, 2005; Chowdhury *et al.*, 2008; Kumar *et al.*, 2008; Bhattacharya and Das, 2007; Wang *et al.*, 2003). In general, increase in rf power increased the dissociation of SiH_4 and H_2 thus increasing the number of SiH_x (x = 1, 2, 3) radicals and atomic hydrogen in the plasma (Lin *et al.*, 2003).

This dissociation of SiH_4 and H_2 molecules into SiH_x and H radicals are usually referred to as primary reactions (Lebib and Cabarrocas, 2005; Chowdhury *et al.*, 2008; Kumar *et al.*, 2008; Bhattacharya and Das, 2007). The primary reactions are enhanced with increase in rf power. This process however depletes reactive SiH_4 molecules and thus reduces secondary reaction (Lebib and Cabarrocas, 2005; Chowdhury *et al.*, 2008; Kumar *et al.*, 2008; Bhattacharya and Das, 2007; Wang *et al.*, 2003). This reaction is due to energetic collisions of SiH_x and H radicals with SiH_4 molecules forming more SiH_x and H radicals. The SiH_3 radicals which have the longest lifetime as they do not participate in secondary reaction are the main growth precursors. Secondary reaction increases the population of SiH_3 radicals reaching the film growth sites. Increase in rf power depletes SiH_4 molecules, thus reducing the number of SiH_3 radicals reaching film

growth sites. On the other hand, increase in rf power also enhances the presence of energetic hydrogen atom reaching the growth surface. The hydrogen etching effects preferentially remove weak or strained Si–Si bonds resulting in formation of Si dangling bonds. The increased presence of atomic hydrogen enhances the surface diffusion of hydrogen atoms thus increasing the presence of hydrogen terminated bonds. The growth surface reactions in the form of abstraction of these Si-H bonds by the SiH_3 radicals and diffusion of SiH_3 radicals on to these nucleation sites increases the growth rate. Competition between these processes influences the growth rate of the Si:H films.

For CD film, the slow increase in growth rate up to rf power of 60 W was contributed by the increase in the growth radicals reaching the growth sites with increase in rf power. This is due to the increase in dissociation of SiH_4 and H_2 molecules. This effect increases the number of SiH_x (x = 1, 2, 3) and H radicals reaching the substrates resulting in competition between film growth and hydrogen etching processes. For films deposited at rf power above 60 W, the slow growth rate with increase in rf power indicated that film growth rate was slightly higher than hydrogen etching process. Increase in rf power above 60 W may lead to high dissociation of SiH_4 molecules. This reduced secondary reactions thus reducing the number of growth radicals reaching the substrates resulting in equilibrium between the rate of film growth and creation of growth sites.

As for the LBL films, the influence of rf power produced a reversed trend compared to the CD films. This showed that the periodical interruption of the film growth process with hydrogen plasma treatment produced reversed effects on growth kinetics of the Si:H films. The high growth rate of the LBL film at the lowest rf power of 20 W showed that during hydrogen plasma treatment, hydrogen etching effect created an optimized number of growth sites in the form of hydrogen terminated bonds for the number of SiH_3 radicals present at these growth sites during the film growth

process at this rf power. These processes were repeated during the next cycle of the hydrogen plasma treatment and film growth thus significantly increasing the growth rate. The decrease in growth rate with increase in rf power to 60 W may be due to the higher number of growth sites created during the hydrogen plasma treatment compared to the number of growth radicals available for film growth. Increase in rf power increased the dissociation of hydrogen molecules thus increasing the number of hydrogen atoms at the growth sites during the hydrogen plasma treatment process but reduced the number of SiH_3 radicals as secondary reactions in the gas phase were reduced. The shorter residence time of the gas molecules in the reaction chamber during the deposition cycle also contributed to reduces the number of SiH_3 radicals reaching the growth sites as the rf power was increased as secondary reaction was reduced. The saturation of the growth rate for rf powers above 60 W which coincided with the saturation of growth rate of the CD film suggested that at this rf power hydrogen molecules were almost completely dissociated at this rf power. This reduced hydrogen etching effects during both film growth and hydrogen plasma treatment processes in the LBL film growth. This resulted in an equilibrium number of growth sites created and SiH_3 radicals available at these sites during the film growth process producing the saturated growth rate with increase in rf power. The presence of SiH_3 radicals was also reduced at these rf powers as secondary reactions were reduced due to almost complete dissociation of precursors gases. This also contributed to the low constant growth rates at these rf powers.

Figure 4.3(b) showed that deposition rate of the LBL films gradually increased from 2 to 6.6 Å/s with increase in substrate temperature from room temperature to 400°C. Similar to the effects of rf power on the growth rate of Si:H film, the deposition rate of the CD films showed a reverse trend with T_s, compared to the LBL film. The film growth rate gradually decreased from 8.4 to 4.2 Å/s with increase in substrate

temperature from room temperature to 400°C. The growth rates of the LBL film was also observed to be significantly lower compared to the CD films for the films prepared at room temperature, T_s of 100 and 200°C.

Usually, substrate temperature is one of the important parameters, which controls the surface reactions and the growth kinetics (Hadjadj *et al.*, 2001; Jadkar *et al.*, 2007; Bhattacharya and Das, 2008). Increase in substrate temperature increases the mean free path of radicals in the plasma and this reduces the probability of collisions with molecules in the plasma. This reduces secondary reactions and decreases the number of SiH_3 radicals, the main growth precursors and hydrogen atoms reaching the substrates. The increase in surface mobility of growth precursors and hydrogen atoms at higher T_s also results in large diffusion coefficient of these radicals and this contributes to a more ordered film structure. Increase in the hydrogen evolution rate along with thermal annealing effects at higher T_s remove weakly bonded species from the growth sites. The above combined effects produced the decreasing growth rate trend with increase in substrate temperature for the CD films and these films are expected to have a more ordered film structure. The dominant presence of hydrogen terminated bonds produced during the hydrogen plasma treatment process at low substrate temperature prevented increase in growth rate during the film growth process for the LBL film grown at low T_s. Increase in T_s during the hydrogen plasma treatment increased the number of nucleation sites as a result of increase in the surface mobility and diffusion coefficient of the hydrogen atoms. This increased the growth rate at the onset of the film growth process cycle. These processes were repeated during the next cycle of the hydrogen plasma treatment and film growth processes thus significantly increasing the film growth rate of the LBL films.

Figure 4.3(c) showed that deposition rate of the LBL films increased to a maximum of 10 Å/s for films prepared at R of 8 and decreased again to a saturation

value for the film deposited at *R* of 16 and 20. The deposition rate remained constant at 5.2 Å/s for the films prepared at these *R* values. The deposition rate for the CD films increased to a high value for the film prepared at *R* equals to 16 and dropped significantly to 3.5 Å/s for the film prepared at *R* of 20.

In this work, *R* is changed by increasing the hydrogen flow-rate at fixed silane flow-rate. Increase in the hydrogen dilution correspondingly reduces the SiH_x radicals in the gas phase and at the growth sites. However, the increase in hydrogen dilution has the effect of increasing the presence of hydrogen atoms at the growth sites which correspondingly enhances hydrogen etching effects. The increase in growth sites produced by hydrogen etching effects is expected to increase the growth rate if sufficient growth radicals are present to diffuse onto these created growth sites. Thus, if the number of growth sites created is larger than the number of growth radicals present for diffusion onto these sites, the growth rate is expected to drop. The high maximum deposition rate obtained for the CD films prepared at *R* equals to 16 may be attributed to the longer residence time for the SiH_x radicals in the deposition chamber allowing for more secondary gas phase reactions thus increasing the number of growth radicals reaching the growth sites created by the hydrogen etching effects. The hydrogen plasma treatment process for the LBL films created larger number of growth sites but the number of radicals reaching the growth sites were smaller as the deposition process was fixed only for 5 minutes. Possibility of occurrences of secondary gas phase reactions is lower thus reducing the number of the radicals reaching the growth sites. This explains the lower maximum deposition rate of the LBL film prepared at *R* equals to 8 compared to the maximum deposition rate of the CD film prepared at *R* of 16.

The results showed that in CD process, the growth and nucleation takes place at the same time at the growth surface and plasma process has significant influence on nucleation. In LBL process, nucleation is mainly induced by the hydrogen plasma

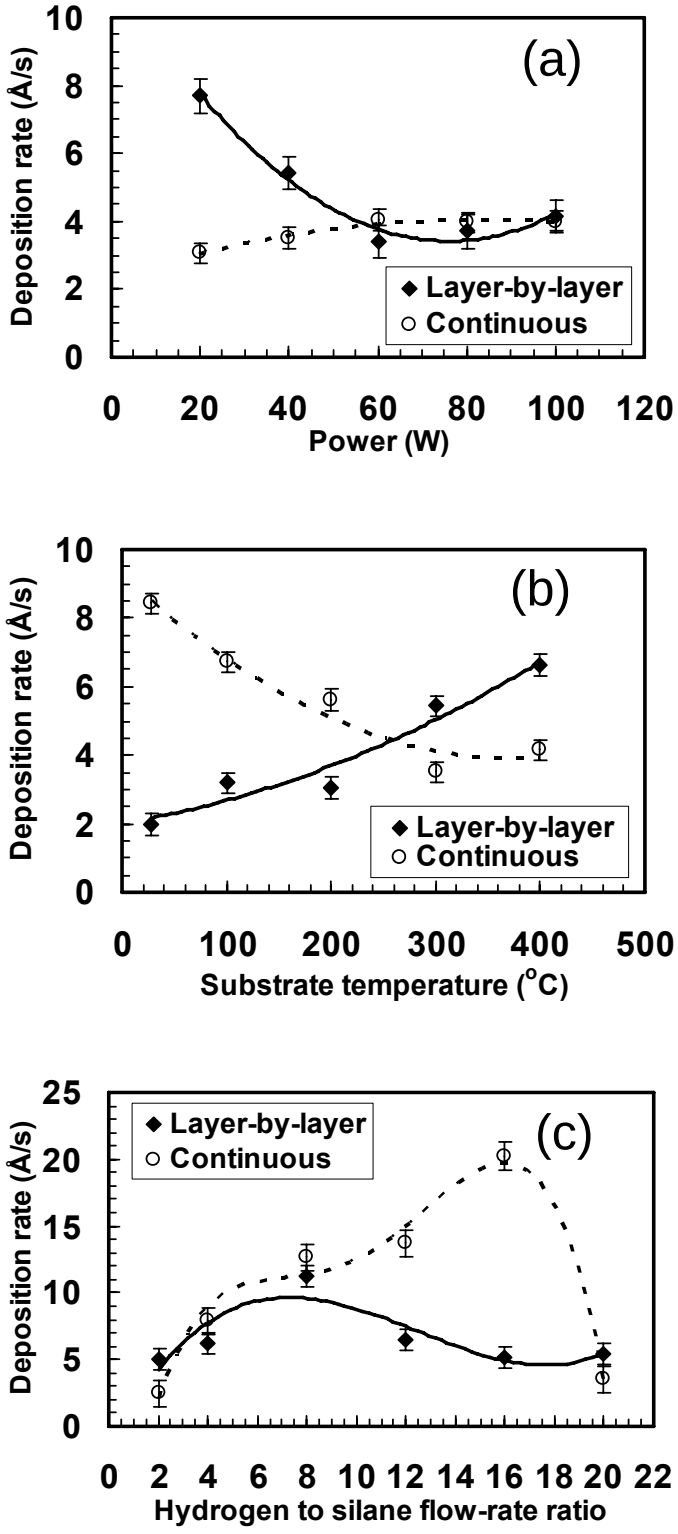

Figure 4.3: Variation of deposition rate of the films with applied (a) rf power, (b) substrate temperature, T_s and (c) hydrogen to silane flow-rate ratio, R.

treatment thus nucleation does not depend critically on the plasma properties during the deposition process. This explains the reversed trends of the growth rate with respect to rf power and substrate temperature.

4.2.2 Refractive Index

The refractive indices of the films studied in this work were obtained from interference fringes of optical transmission spectra using Manifacier and Davies techniques combined as described in Section 3.3.1.1. Figure 4.4 shows the Cauchy plots of refractive index as a function of wavelength for Si:H films studied in this work in the wavelength range of the spectra of the films where the interference fringes were observed. The refractive indices of the films showed almost no dependence on the wavelength in the non-absorbing region ($\lambda > 1700$ nm). Significant dispersion in the refractive indices of the films was observed in the absorbing region. The trends of the variations of the refractive indices with rf power, T_s and R showed differences in the non-absorbing region and the absorbing region as a result of changes in the gradient of the slopes of dispersion curves of the refractive index in the absorbing region.

The static refractive index, n_0 is estimated by extrapolating the spectral refractive index to the non-absorbing long wavelength region where $\frac{A}{\lambda^2} \to 0$. The variations of n_0 with rf power, T_s and R are shown in Figure 4.5(a), (b) and (c) respectively. Increase in refractive index has been related to increase in compactness of a film structure and reduction in the number of microvoids (Tang *et al.*, 2009; Millerova *et al.*, 2010). However, low refractive index is also indicative of high hydrogen content in the film structure.

Figure 4.5(a) showed the n_0 of the LBL films increased significantly from 2.88 to 3.7 with increase in rf power from 20 to 40 W. This n_0 value decreased with further

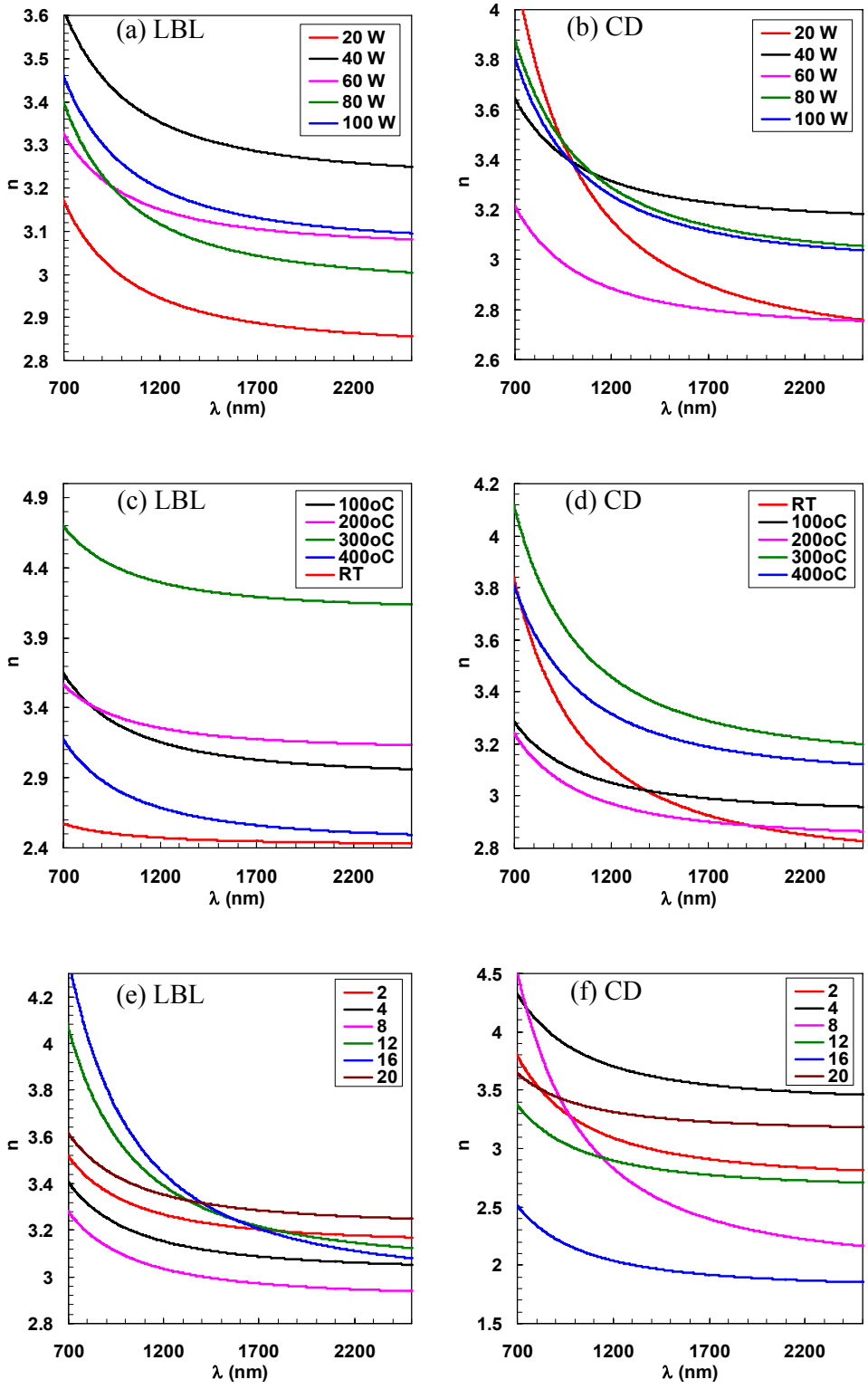

Figure 4.4: Variations of n against λ for the LBL and CD films deposited at different rf powers (a) and (b), substrate temperatures, T_s (c) and (d) and hydrogen to silane flow-rate ratios, R (e) and (f) respectively.

increase in rf power to 60 W and showed no change with increase in rf power to 100 W. Increase of refractive index of the LBL and CD films at low rf power of 40 W indicated formation of compact structure in the films with sufficient hydrogen etching but the effect was shown to be more significant for the LBL film. This suggested that the periodical hydrogen plasma treatment of the growing surface enhanced hydrogen etching effect which led to the formation of a more compact film structure. Further increase in rf power for the LBL film however led to an increase in incorporation of hydrogen into the films structure resulting in the decrease the film density. During the hydrogen etching process, growth sites were created but with the increase in number of hydrogen atoms, the number of hydrogen terminated bonds was also increased. A similar trend was observed for the film prepared at rf powers between 20 to 60 W for the CD films but a second increase in n_0 value was observed for the films with further increase in rf powers. The higher presence of weak Si-Si bonds as a result of increased dissociation of silane and reduction in secondary gas phase reactions at these rf powers enhanced hydrogen etching effects with increase in presence of hydrogen atoms at these high rf powers.

Figure 4.5(b) showed the refractive index of the LBL films increased significantly from 1.95 to 3.7 with increase in substrate temperature to 300°C. The refractive index of the films decreased to 2.49 with further increase the substrate temperature to 400°C. Increases in substrate temperature increased the thermal annealing effect of the growth surface during the hydrogen plasma treatment of the LBL film prepared at T_s of 300°C. This may contribute to a more compact and more ordered film structure thus increasing n_0. The decrease in the n_0 value for the LBL film prepared at 400°C showed that evolution of hydrogen at this T_s increased the number of dangling bonds forming voids in the film structure. This contributed to the decrease in the density of the film and correspondingly n_0 of the film. The n_0 value for the CD films showed

almost no dependence on T_s. This can be due to the equilibrium between the thermal annealing and hydrogen etching effects with incorporation of Si atoms in the film structure as a result of longer residence time of the radicals in the chamber during the growth process. This also contributed to films with higher hydrogen content thus the n_0 values were maintained close to 3 at all T_s.

Figure 4.5(c) showed the n_0 values of the LBL films were around 3 for the films prepared at R below 16 and increased to 3.7 with further increase in R of 20. The CD films showed that the n_0 values decreased to a minimum from 3 to about 1.8 with increase in R to 16 and increased again to 3 with increase in R to 20. Increase in R to 16 for the CD directly increased hydrogen incorporation or voids in the film structure thus producing less dense films. The increase in n_0 values at the highest R for the CD film could be due to enhancement in hydrogen etching effects which increased the structural order of the film. The periodic hydrogen plasma treatment during the LBL deposition process retained the n_0 values within the values close to refractive index of c-Si of 3.4 (Halindintwali, 2005) indicating that the films were more ordered in structure. The increase in the n_0 values to 3.7 for the film prepared at the highest R may indicate that the increased hydrogen etching process also improved structural ordering in the film structure resulting in a denser film structure.

4.2.3 Optical Energy Gap

In this work, optical energy gap, E_G is determined using the Tauc relation as described in Section 3.3.1.2. This relation of determining E_G of amorphous and indirect band gap semiconducting films is widely used by most researchers (Guo *et al.*, 2011; Bhattacharya and Das, 2008; Luo, *et al.*, 2008; Bhattacharya and Das, 2007). By plotting the graph $(\alpha E)^{1/2}$ against photon energy, E, E_G is obtained from the intersection of the linear part of the curve extrapolated onto the E-axis. Figure 4.6

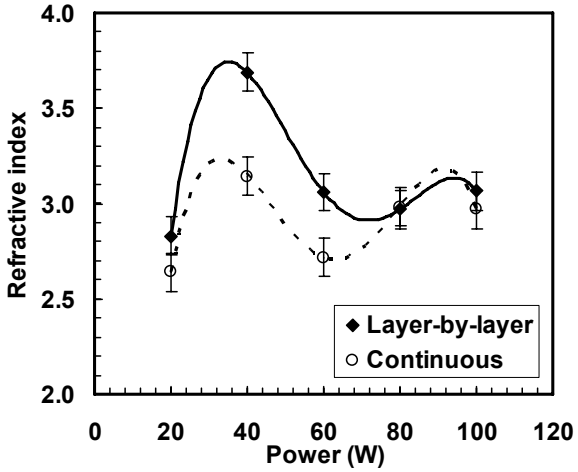

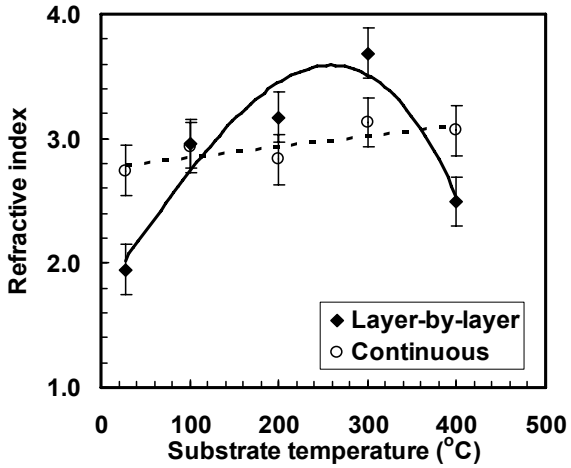

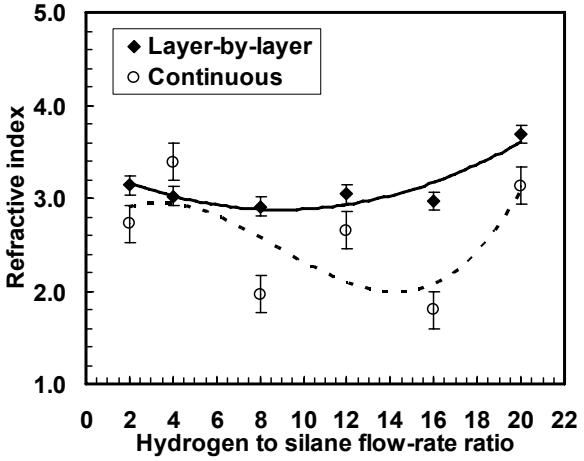

Figure 4.5: Variation of refractive index of the films with (a) rf power, (b) substrate temperature, T_s and (c) hydrogen to silane flow-rate ratio, R.

shows a typical Tauc plot for Si:H thin films deposited at different rf powers with substrate temperature and hydrogen to silane flow-rate ratio were fixed. The curves of $(\alpha E)^{1/2}$ against photon energy for the LBL and CD films deposited at various rf power, T_s and R are shown in Figure 4.7.

For the film deposited by PECVD, the change of E_G of Si:H thin film is usually related to either the hydrogen content in the film or the quantum confinement effect due to the presence of nano-sized Si nano-crystallites embedded within an amorphous matrix (Jadkar *et al.*, 2002; Ali, 2007; Remolina *et al.*, 2009). It has been established in many reported works that incorporation of hydrogen into the film structure passivates dangling bonds thus removing defects and this has the effect of widening E_G (Jadkar *et al.*, 2002). Incorporation of hydrogen at the threshold of crystallinity enhances the formation of nucleation sites and through abstraction and diffusion processes by SiH_3 radicals, the structural order of the film can be improved and lead to the formation of nanocrystalline structures in film (Ali, 2007; Remolina *et al.*, 2009). The former can lead to formation of a homogeneous structured of amorphous Si:H film and the latter

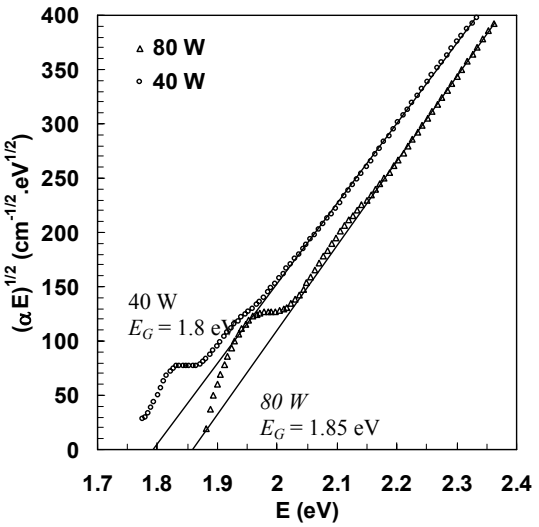

Figure 4.6: Typical Tauc plot of $(\alpha E)^{1/2}$ against photon energy, E for Si:H thin films deposited at different rf powers.

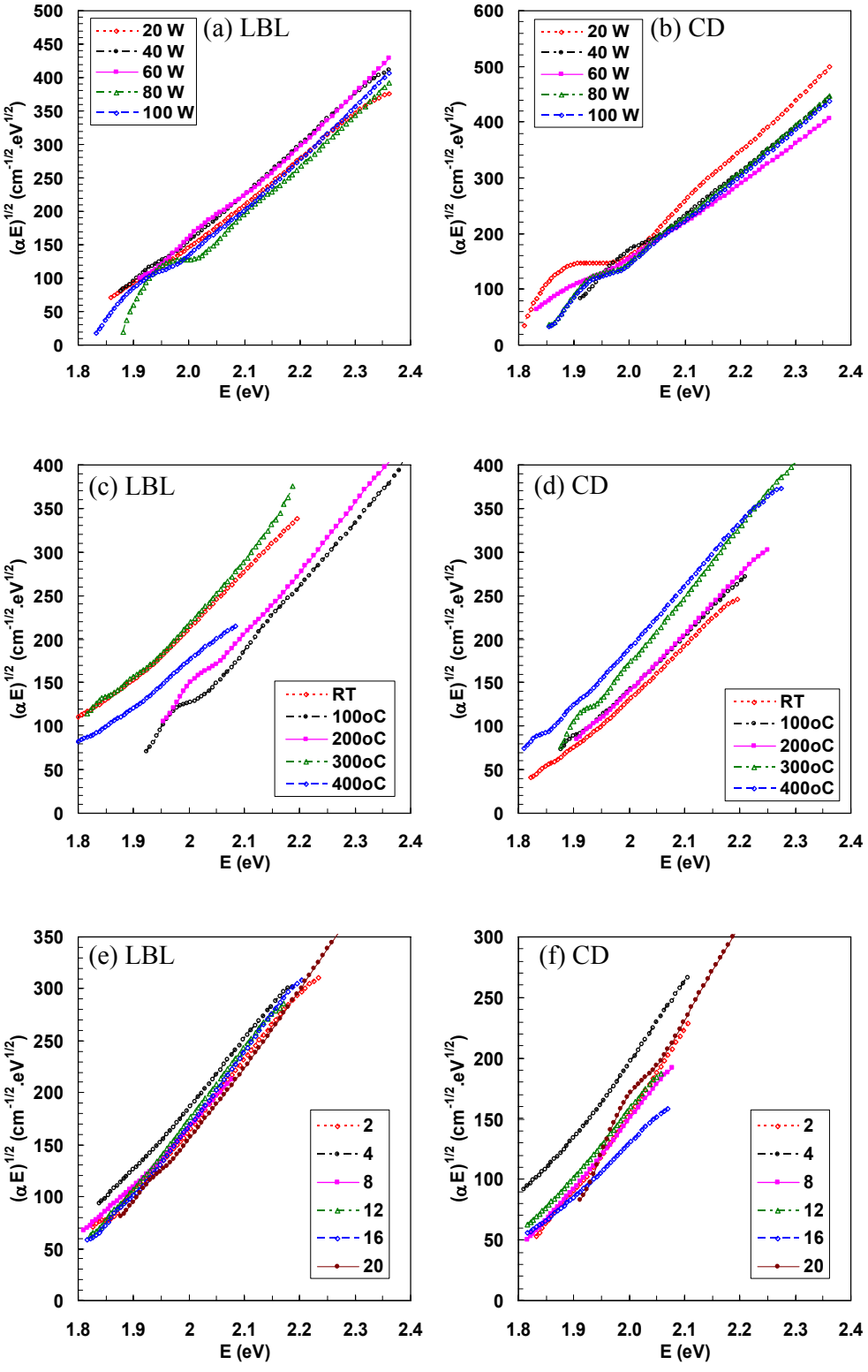

Figure 4.7: $\sqrt{\alpha hv}$ as a function of photon energy for the LBL and CD films deposited at different rf powers (a) and (b), substrate temperatures, T_s (c) and (d) and hydrogen to silane flow-rate ratios, R (e) and (f) respectively.

can lead to the formation of multiphase structured of Si:H film consisting of nanocrystallites embedded within an amorphous matrix. Figure 4.8 shows the variations of E_G with rf power, T_s and R respectively for both LBL and CD thin films studied in this work. The values of E_G recorded for all films were in the range of 1.65 to 1.87 eV. It is interesting to note that the LBL films produced significant variations in E_G values at different rf powers and T_s. The E_G of CD films showed small variations with rf power, T_s and R. This indicates that the CD films are mainly amorphous and these deposition parameters have no significant influence on the crystallinity of the films. The variation of E_G for the CD films with rf power, T_s and R was only between 1.75 to 1.85 eV. This range of small E_G value is usually observed in cases where E_G shows strong influence on the hydrogen content. The large variation of E_G with deposition parameters is usually due to the change of crystallinity in the film often contributed by the presence of nanocrystallites embedded within an amorphous matrix. This produces quantum confinement effects and decrease in crystallite size has been reported to widen E_G (Das, 1995). Low hydrogen content and decrease in structural order in Si:H films narrows E_G.

The variation of the optical energy gap, E_G against rf power for the LBL and CD films is shown in Figure 4.8(a). The E_G for the CD films showed slight decrease with increase in rf power to 40 W and remained unchanged with increase in rf power above 40 W. The E_G for the LBL films showed an increasing trend with increase in rf power to 60 W and remained constant with further increase in rf power. The small change in E_G for the CD films could be due to very little change in hydrogen content or crystallinity in the films. The effects of rf power on E_G appeared to be reversed compared to the effects of growth rate in Figure 4.4(a) for both the LBL and CD films. Complete dissociation of SiH_4 molecules and increased dissociation of H_2 molecules at higher rf power increased secondary reaction of SiH_x radicals with H_2 molecules and this reduced the number of H atoms reaching the growth sites resulting in lower hydrogen content

films. The complete dissociation of the SiH_4 molecules resulted in films with constant hydrogen content at high rf power. This reduced the E_G of the films to a saturation value with increase in rf power to 40 W for the CD films. For the LBL films, the increase in rf power increase the energy of the H atoms reaching the plasma thus enhancing hydrogen etching effects during the hydrogen plasma treatment. This increased the number of H passivated bonds at the onset of the deposition process. The SiH_3 radicals reaching the growth sites also decreased with complete dissociation of the SiH_4 molecules and this contributed to increase in hydrogen content in the films to a saturation value. The increased in hydrogen content in the films may contribute to the increase in E_G in LBL film to a saturation value at rf power of 60 W. The significant increase in E_G compared to the CD films suggested that quantum confinement effects also may have produced the broadening of E_G (Das, 1995). The presence of Si nano-crystallites embedded with an amorphous matrix of the film may also contribute to this effect.

The variation of E_G against T_s for the LBL and CD films is shown in Figure 4.8(b). For the LBL films, the E_G increased significantly from 1.65 eV to a maximum of 1.85 eV with increase in substrate temperature from room temperature to 100 and 200°C. The significantly increase in E_G for the LBL film prepared at these T_s was most likely contributed either by increase in hydrogen incorporation or quantum confinement effects. The periodic hydrogen plasma treatment process may enhance hydrogen incorporation and also hydrogen etching effects. Hydrogen etching effects can lead to the formation of Si nano-crystallites within the film structure and produce quantum confinement effects. The E_G decreased with increase in T_s for the films prepared at T_s above 200°C. The increase in T_s may increase the size of Si nano-crystallite or decrease in hydrogen incorporation in the film structure. The former may explain the decrease in E_G for the film prepared at 300°C and the latter is most likely to contribute to the decrease in E_G for the film prepared at 400°C. Almost no change was observed in E_G for

the CD films with increase in substrate temperature to 300°C. This shows that there is almost no structural change in the CD films when prepared at these T_s. The E_G of CD film showed a small decrease with increase in substrate temperature to 400°C. The slight decrease of the E_G for the CD film prepared at 400°C can be due to low incorporation of hydrogen into the film structure at this temperature.

The variations of E_G against R for the LBL and CD films are shown in Figure 4.8(c). The R appeared to produce a noticeable influence on E_G of the CD films compared to the LBL films. For the CD films, the values of E_G are high (~1.8 eV) for the films deposited at lowest and highest R of 2 and 20 respectively. The E_G remained at values between 1.69 and 1.73 eV for the films deposited at R of 4 to 16. For the LBL films, the E_G however showed a different trend in the variation of E_G with R. The range of E_G values varied between 1.7 to 1.76 eV with change in R from 2 to 20. Increase in E_G can be related to increase of hydrogen incorporation in the film structure or quantum confinement effect. High values of E_G were registered for the films deposited at the lowest R of 2 for both CD and LBL films. The lower pumping rate of the reactor to maintain similar deposition pressure as the other films deposited at higher R allowed longer residence time for the growth radicals and H atoms at the growth sites. This enhanced hydrogen etching effects during the hydrogen plasma treatment, and abstraction and diffusion process of SiH_3 during the growth process in the LBL films and both processes were enhanced simultaneously during the growth process of the CD films. This may result in the formation of Si nano-crystallites embedded within an amorphous matrix and the larger E_G for this film maybe due to quantum confinement effect. At the highest R for the CD film, the higher concentration of H molecules in the reactor increased the incorporation of hydrogen into the film structure thus increasing E_G. The decrease in the effectiveness of H etching effect as a result of shorter residence time of radicals and H atoms in the plasma retarded the formation of an ordered film

structure in the CD films deposited at R of 4 to 16. This has the effect of decreasing E_G for this film. However, the increase in concentration of H atoms reaching the substrates contributed increased H incorporation in the film. The equilibrium between these two competing processes explained the the almost constant E_G for these films.

The B determined from Tauc relation refers to the edge width parameter. B indicates the sharpness of the band edge and is related to the width of band tails or disorder of the film. Usually, a higher value of B indicates more ordered film structure (Bhattacharya and Das, 2008). Wang *et al.* reported in their work on a-Si:H/nc-Si:H thin films that presence of Si nano-crystallites within an amorphous matrix increases the E_G and B values. The B value represents the structural order of this multiphase structured and is dependent on the homogeneity of the film. Figure 4.9 shows the variations of B with rf power, T_s and R for the LBL and CD thin films. It was noted that both of the LBL and CD films showed large variations in B values (from 421 – 978 $cm^{-1/2}.eV^{-1/2}$) at different rf powers, T_s and R. Higher value of B indicated increase in the structural order in the film.

Figure 4.9(a) shows that rf power has significant influence on the structural order of the film structure. CD films prepared at the lowest rf power of 20 W has the highest B value of about 1000 $cm^{-1/2}$ $eV^{-1/2}$ indicating highest structural order compared to the other films studied in this work. Increasing rf power to 60 W resulted in CD film with the lowest B. CD films prepared at high rf powers of 80 and 100 W resulted in moderate structural order in films with B values close to 800 $cm^{-1/2}$ $eV^{-1/2}$. The LBL films showed the lowest B value when prepared at the lowest rf power and increase in rf power to 60 W produced film with the highest B value. The B value of the films prepared at 80 and 100 W however increased to a saturation value of similar moderately ordered film as the CD films prepared at the same rf powers.

Thus, the results indicated that the CD film prepared at the lowest rf power had

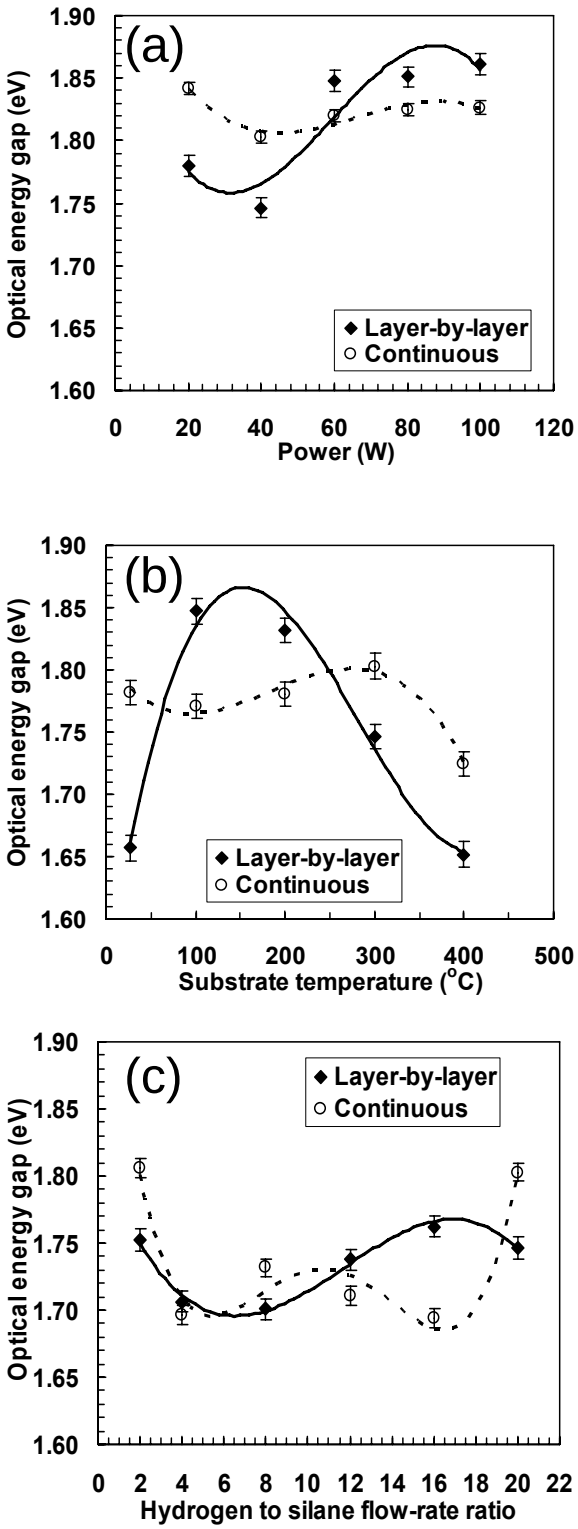

Figure 4.8: Variation of optical energy gap of the films with (a) rf power, (b) substrate temperature, T_s and (c) hydrogen to silane flow-rate ratio, R.

the most ordered film structure. The corresponding large E_G of this film also suggested that the film has a possible structure of Si nano-crystallites embedded in an amorphous network. The long residence time of the radicals in the reactor during CD deposition compared to the LBL deposition allowed higher frequency of secondary reaction thus increasing the number of SiH_3 radicals reaching the growth sites. This could contribute to the formation of the nanocrystalline film structure in the film. The moderately high structural order of the films prepared at high rf powers of both CD and LBL films strongly indicated that hydrogen etching effects contributed to this effect. The hydrogen etching effects at these rf powers may induce onset of crystallization in the film structure resulting in mixed phases of amorphous and nanocrystalline in the film structure. These mixed phases may have resulted in the lower B value compared to the highly ordered amorphous phase of the CD film prepared at low rf power.

T_s showed significant influence on the structural order of the film structure [Figure 4.9(b)]. Similar mixed phases of amorphous and nanocrystalline may be formed in CD films prepared at high substrate temperatures of 300 and 400°C. The LBL films prepared at 100 to 300°C showed structural order of the same order of magnitude as the CD films prepared at the two highest T_s indicating highest structural order. This showed that hydrogen etching effects during the hydrogen plasma treatment was most effective at these T_s in LBL films. High T_s of 400°C failed to incorporate enough H saturated bonds at the onset of the deposition process in LBL deposition resulting in less effective H etching effect for formation of highly ordered films. The longer residence time of radicals and H atoms at the growth sites produced more ordered film structure of CD films prepared at the highest T_s of 400°C.

The variation in B with R [Figure 4.9(c)] appeared to replicate the variation in refractive index of the films with R [refer to Figure 4.5(c)]. The B values of the LBL films were around 600 $cm^{-1/2}$ $eV^{-1/2}$ for the films prepared at R below 12 and increased

to about 800 $cm^{-1/2}$ $eV^{-1/2}$ with further increase in *R* to 20. The CD films showed that the *B* values decreased to a minimum from 800 $cm^{-1/2}$ $eV^{-1/2}$ to about 400 $cm^{-1/2}$ $eV^{-1/2}$ with increase in *R* to 16 and increased again to 800 $cm^{-1/2}$ $eV^{-1/2}$ with increase in *R* to 20. Increase in *R* to 16 for the CD directly increased hydrogen incorporation or voids in the film structure thus producing less ordered film structure. The increase in *B* value at the highest *R* for the CD film could be due to enhancement in hydrogen etching effects which increased the structural order of the film. The slow increase in the *B* value with increase in *R* to the highest *R* of 20 may indicate that the increased hydrogen etching process improved structural ordering in the film for the LBL film.

4.3 Fourier Transform Infrared (FTIR) Spectra

The infrared spectrum provides information on the structural and chemical bonding configurations of the Si:H thin film. In this work, the infrared spectrum was used to study the Si-H vibrational modes of absorption bands which are related to the hydrogen distribution and local bonding configurations (Han and Wang, 2003). In the Si:H thin film, hydrogen plays a crucial role in determining the structural phase transition in the material. Therefore, Si-H absorption bands of the Si:H thin films were the main study in this work. Generally, infrared spectrum of Si:H thin film consists of three important absorption bands which are related to Si-H bonding configuration. The absorption peak at 630 cm^{-1} is related to the Si-H wagging mode, a doublet at 850 and 890 cm^{-1} is related to $Si-H_2$ bending modes, and the absorption peak between 2000 and 2090 cm^{-1} is related to Si-H stretching and $Si-H_2$ stretching modes respectively (Pollard *et al.*, 1982; Langford *et al.*, 1992; Cardona, 1983; Lucovsky and Pollard, 1984; Manfredotti *et al.*, 1994). Figure 4.10 shows an typical spectrum of FTIR for Si:H thin film produced by PECVD.

In this work, the infrared transmission spectra of the films were obtained using a

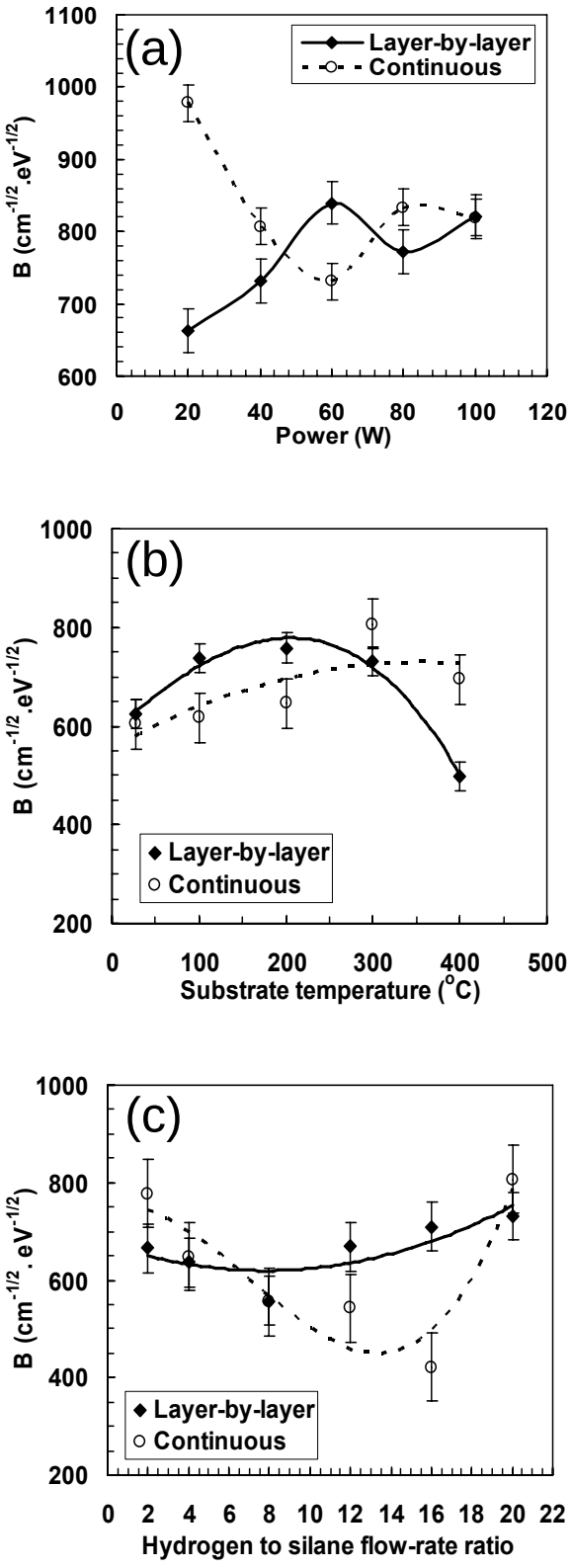

Figure 4.9: Variation of B of the films with (a) rf power, (b) substrate temperature, T_s and (c) hydrogen to silane flow-rate ratio, R.

Fourier transform infrared (FTIR) spectrometer (Perkin-Elmer System 2000) in the range of 4000 to 400 cm^{-1}. This characterization was done on the films deposited on c-Si substrate because c-Si is not infrared active to first order because of the tetrahedral symmetry. Also, it will not have any infrared absorption spectrum due to silicon hydrides modes. Any hydrogen contamination is well below the spectrometer detection limit. The FTIR transmission spectra for the LBL and CD films deposited at different rf powers, substrate temperatures, T_s and hydrogen to silane flow-rate ratios, R are divided into the three main absorption bands related to the Si-H bonding configurations. The absorption coefficient normalized to the film thickness are calculated in these regions and subtracted with the linear baseline and detail analysis of these absorption spectra are presented and discussed in the following sections

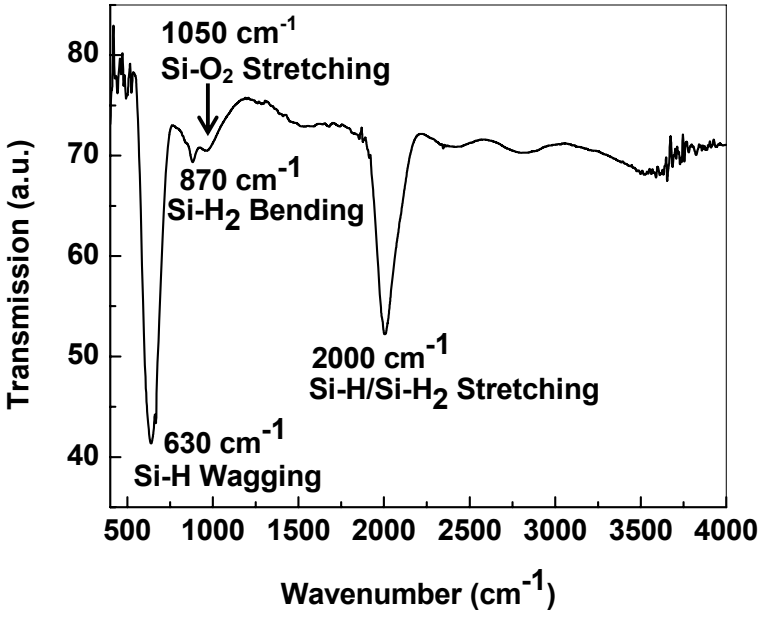

Figure 4.10: Typical FTIR spectra of Si:H thin film deposited by rf PECVD.

4.3.1 Analysis of Absorption Bands in the Region of 500 - 700 cm^{-1}

Figure 4.11 shows the normalized absorption spectra in the Si-H wagging mode region between 500 to 800 cm^{-1} for the LBL and CD films deposited at various rf powers, T_s and R. The Si-H wagging band at 630 cm^{-1} is usually related to the total bonded hydrogen content in the film (Bhattacharya and Das, 2007; Cheng *et al.*, 2009).

The bonded hydrogen content, C_H in the Si:H thin films is calculated from these absorption bands using the following equation presented in Section 3.3.2.3. Curve fittings of the bands are performed on a Gaussian distribution peak using Origin Pro version 8.1 and the integrated intensities of these peaks are then calculated. Inserting the integrated intensity into Equation 3.22, C_H for the films is determined. The variations of hydrogen content, C_H against rf power, T_s and R for the LBL and CD films are shown in Figure 4.12(a), (b) and (c) respectively. Hydrogen incorporation into Si:H thin film structure has significant influence on the performance of Si-based devices. From various reports (Cheng *et al.*, 2009), for solar cell photovoltaic applications C_H of less than 10 % in Si:H films is favoured because degradation by Staebler-Wronski effect is reduced for stable operation of Si-based thin film solar cells.

Figure 4.12(a) shows that the C_H of the LBL films remained constant at about 10 % with increase in rf power from 20 to 40 W. The value of C_H increased significantly with further increase in rf power to 100 W. For the CD films, the C_H values fluctuated between 13 to 20 % with increase in rf power. The lowest value was registered for the film prepared at rf power of 40 W. C_H for the CD film showed similar increasing trend as the LBL films with increase in rf power from 40 to 80 W although registering a lower value. For continuous deposition using conventional rf PECVD, increase in rf power increased the dissociation rate of SiH_4 and H_2, thus increasing the number of radicals (SiH_3, SiH_2, etc), atomic hydrogen and ions in the plasma (Das and Ray, 2002). This enhances the probability of more energetic hydrogen atoms reaching the growth

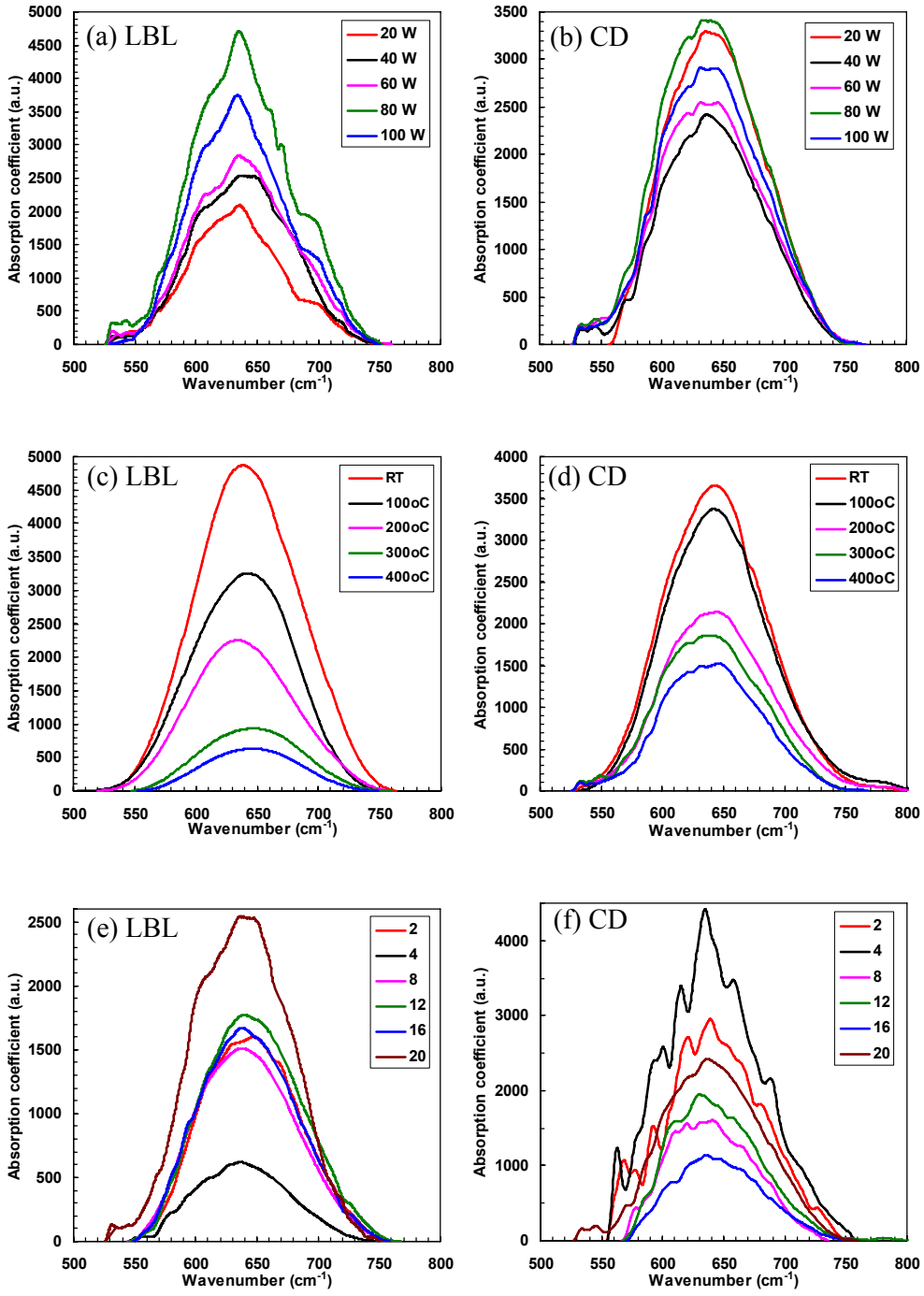

Figure 4.11: Absorption coefficient at 630 cm^{-1} for the LBL and CD films deposited at various rf powers (a) and (b), substrate temperatures, T_s (c) and (d) and hydrogen to silane flow-rate ratios, R (e) and (f) respectively.

surface through secondary reactions with undissociated SiH_4 molecules. Meanwhile, the hydrogen etching effects preferentially removed weak or strained Si–Si bonds resulting in formation of Si dangling bonds. The increased presence of atomic hydrogen enhanced the surface diffusion of hydrogen atoms onto these dangling bonds thus increasing the presence of Si-H bonds. This explains the increasing trend of the C_H values for the CD films prepared at rf power above 40 W. The similar increasing trend for the C_H values for the LBL films prepared in the same range of rf powers also can be supported by this explanation and the higher C_H recorded for the LBL films was contributed by the incorporation of H atoms during the hydrogen plasma treatment. The slight decrease in C_H for LBL and CD films prepared at rf power of 100 W can be due to depletion of SiH_4 and H_2 molecules in the plasma as a result of complete dissociation resulting in the formation of more dangling bonds. High energy ion bombardments at the highest rf power also led to the lower H atom incorporation in the film. The high C_H value for the CD film on prepared at the lowest rf power maybe due to the low hydrogen etching effects which is effective in lowering hydrogen content in films if the number of SiH_3 growth radicals reaching the growth sites are significantly large. The hydrogen etching effects during the hydrogen plasma treatment of the LBL films totally covered the growing surface with atomic hydrogen. Active abstraction and diffusion by SiH_3 radicals which have the longest lifetime compared to the other SiH_x (x = 1-2) generated in the plasma during the film growth cycle on the hydrogen covered growth surface reduced the number of Si-H bonds in film structure. This contributed to the low C_H film prepared at low rf power for the LBL films.

Figure 4.12(b) shows that T_s has strong influence on C_H in both CD and LBL films. The C_H values decreased with increase in T_s for both films but the rate of change was larger for the LBL films. The T_s of 200°C was the turning point for the transition for the C_H values of the LBL films being larger than the CD films and vice-versa at

higher T_s. It is well documented that the C_H for a-Si:H or nc-Si:H films prepared by continuous PECVD decreased with increase of T_s (Mukhopadhyay *et al.*, 2006; Ray *et al.*, 2002; Matsuda, 2004; Matsuda *et al.*, 2003; Matsuda, 1999). The hydrogen plasma treatment for the LBL process however increased the effectiveness of removing hydrogen from the growth surface at high T_s.

Figure 4.12(c) showed the C_H remained at 10 % for all LBL films prepared at different R except for the film deposited at R of 4 where the value dropped to less than 5%. For the film deposited at the lowest R of 2 the C_H was the highest for the CD film and it decreased to saturation value lower than 10 % with further increase in R. This has been reported in similar work on continuously deposited CD films where increase in R increased the presence of atomic hydrogen at the growth sites which correspondingly increased the hydrogen etching effect. This etched out hydrogen instead of incorporating hydrogen into the network (Mukhopadhyay *et al.*, 2004). Since the C_H in the LBL was observed to be strongly influenced by rf power and T_s these films showed no significant dependence on R.

4.3.2 Analysis of Absorption Bands in the Region of 750 - 1150 cm^{-1}

Figure 4.13 shows the absorption coefficient at 750 - 1150 cm^{-1} for the LBL and CD films deposited at various rf powers, T_s and R. Usually this absorption peak consists of variable vibrational mode components including Si-O-Si in particular local geometries, Si-H_2 bending, Si-O-Si stretching and Si-O stretching modes which are located at 780, a doublet at 840 and 880 , 980 and 1100 cm^{-1} respectively. The presence of oxygen contamination was obviously inevitable in all films. Mullerova *et al.*, 2006, attributed this to post deposition oxidation when exposed to air. For the LBL films deposited at different rf powers, the absorption peaks in this region showed significant appearance of peaks at 780, a doublet at 840 and 880, and 980 cm^{-1} attributed to the Si-

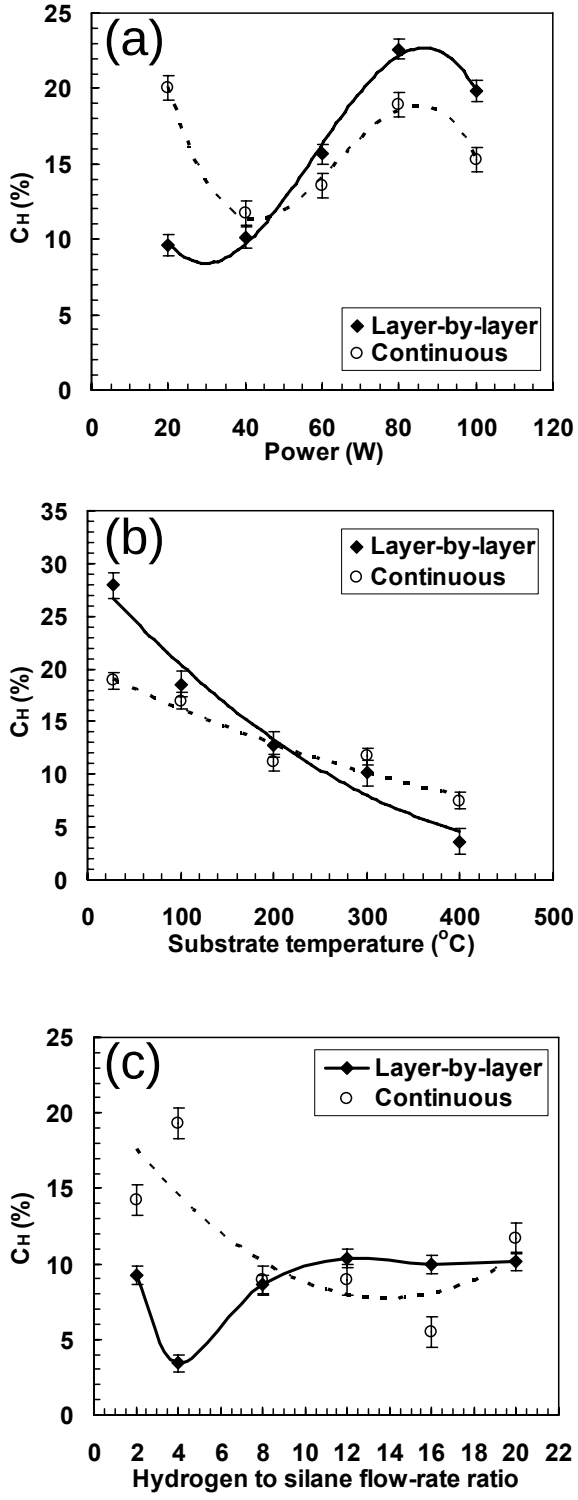

Figure 4.12: Variation of C_H of the films with (a) rf power, (b) substrate temperature, T_s and (c) hydrogen to silane flow-rate ratio, R.

O-Si in particular local geometries, Si-H_2 bending and Si-O-Si stretching modes respectively. The Si-O-Si stretching band is obviously the highest for the films prepared at high rf powers of 80 and 100 W. The higher presence of dangling bonds for these films when exposed to air after the deposition may contribute to this high oxygen contamination. For the CD films deposited at same condition, Si-H_2 bending mode at 840 cm^{-1} was not present and the peaks at 780 and 880 cm^{-1} were not significant. Only the Si-O-Si stretching mode was dominant in these films resulting in the submergence of the Si-H_2 bending modes.

For the LBL films deposited at different T_s [Figure 4.13(b)], a significant trend was observed in the absorption spectra in this range. Two obvious absorption peaks at 880 and 1100 cm^{-1} corresponding to Si-H_2 bending and Si-O stretching modes respectively consistently were present in the spectra of the films prepared at room temperature, 100 and 200°C. The intensity of these absorption peaks decreased and the peak position shifted to lower wavenumber with increase in T_s. The Si-H_2 bending mode disappeared at T_s above 200°C. Correspondingly, oxygen contamination also decreased with increase in T_s. For the CD films, similarly the absorption peaks at 840 and 880 cm^{-1} attributed to the Si-H_2 bending mode were observed in the spectra of films prepared at room temperature and T_s of 100°C but the Si-O stretching band was absent in the spectra of these CD films. These absorption bands significantly decreased in intensity along with the appearance of a small Si-O stretching band in the spectrum of the film prepared at 200°C. The Si-H_2 bending modes at 840 and 880 cm^{-1} disappeared in the spectra of the CD films prepared at T_s of 300 and 400°C as these bands were again submerged by the presence of the large Si-O stretching band. The trend of oxygen contamination appeared to be reversed with respect to the LBL films as high T_s increased oxygen contamination in the film. Hydrogen plasma treatment in the LBL

process at high T_s appeared to be very effective in reducing oxygen contamination in the film structure.

For the films deposited at different R [Figure 4.13(c)], the variation in the absorption spectra in the Si-H_2 bending region did not show much variation with respect to this parameter for both films. The Si-H_2 bending modes at 780 and 880 cm^{-1} in this region were present in all films prepared at different R but were not obvious in the spectra with high absorption intensity of the Si-O-Si stretching band. Therefore, the variations were not observed since deconvolution of this absorption bands were not performed. Obviously, films deposited with low R irrespective whether of the deposition technique had the highest oxygen contamination. The low pumping rate to maintain the required deposition pressure and the low presence of hydrogen atoms in the chamber particularly at the growth surface may contribute to the higher oxygen contamination. Increase in R reduced oxygen contamination for the LBL films but for the CD films, oxygen contamination increased for the film deposited at highest R.

4.3.3 Analysis of Absorption Bands in the Region of 1850 - 2250 cm^{-1}

The variations of absorption coefficient at 1850 - 2250 cm^{-1} for the LBL and CD films deposited at various rf powers, T_s and R against wavenumber are shown in Figure 4.14. This absorption band is due to the overlapping of the Si-H and Si-H_2 stretching bands at 2000 and 2090 cm^{-1} respectively.

The absorption band is deconvoluted into the component Si-H and Si-H_2 stretching bands by fitting them to Gaussian distribution peaks using Origin Pro version 8.1. The integrated intensities of the component peaks were determined and the microstructure parameter, R^* for the films as described in Section 3.3.2.3. R^* represents the degree of disorder associated with the Si matrix (Bhattacharya and Das, 2007). The disorder can be due to the presence of silicon dihydrides or polyhdrides bonds in the

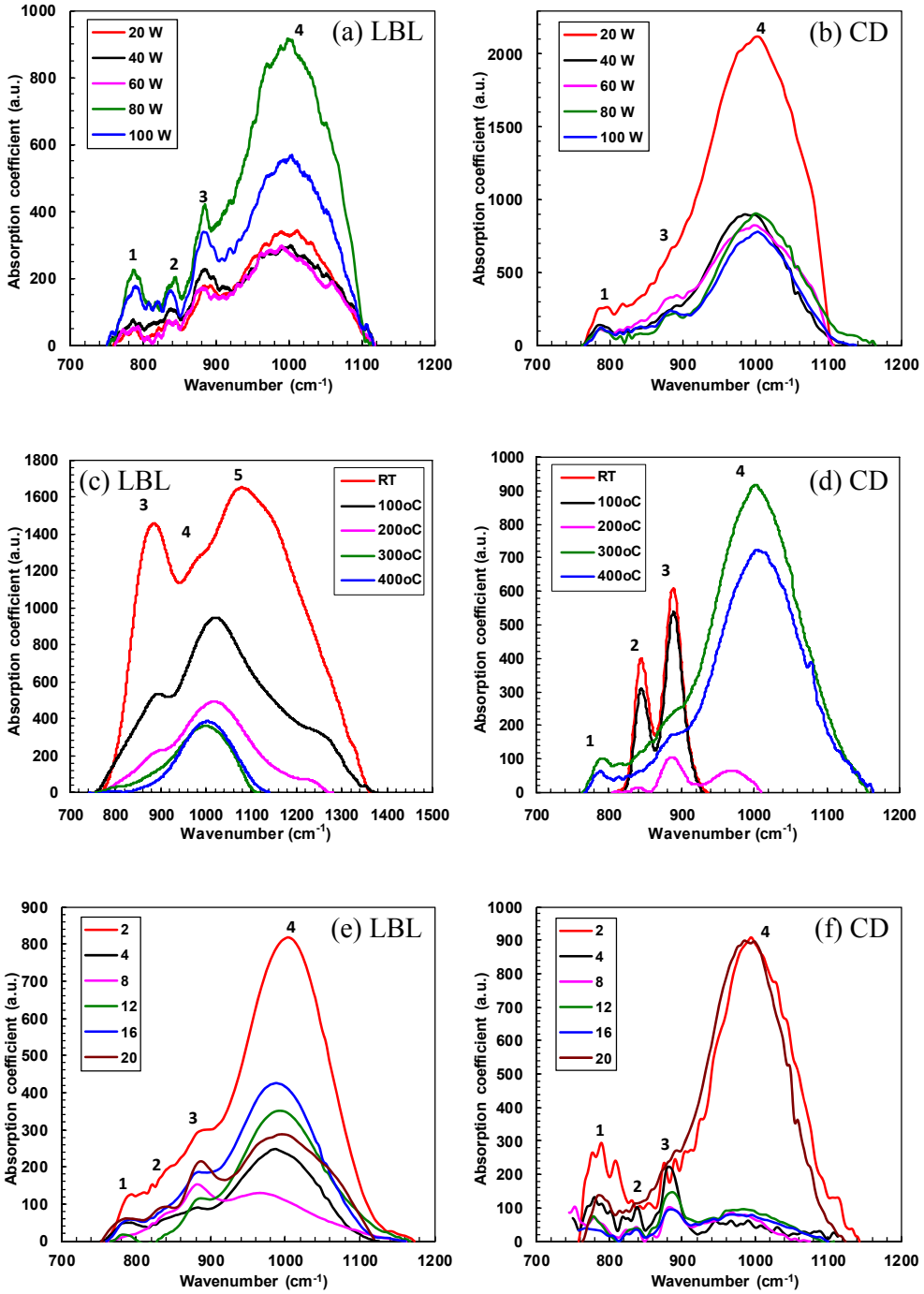

Figure 4.13: Absorption coefficient at 750 – 1150 cm^{-1} for the LBL and CD films deposited at various rf powers (a) and (b), substrate temperatures, T_s (c) and (d) and hydrogen to silane flow-rate ratio, R (e) and (f). The absorption peaks which label as **1**, **2**, **3**, **4** and **5** are correspond to vibrational modes of Si-O-Si in particular local geometries, a doublet of $Si-H_2$ bending, Si-O-Si stretching and Si-O stretching modes, respectively.

amorphous thin film (Bhattacharya and Mahan, 1988; Du *et al.*, 2005). While for μc-Si:H or nc-Si:H thin film, high magnitude of R^* can be associated with the formation of a state of transition from amorphous to crystalline, which has been reported as a highly disordered state of grain boundaries surrounding the Si nano-crystallites formed by high concentration of Si-H_2 bonds (Bhattacharya and Das, 2007; Mukhopadhyay *et al.*, 2004; Chowdhury *et al.*, 2007; Chen *et al.*, 2009). However, with increase in crystallinity and reduction in the disordered grain boundaries, R^* is expected to decrease as a result of increase in structural order in the film structure.

The variations of R^* with rf power, T_s and R for the LBL and CD films is shown in Figure 4.15. The values of R^* for the LBL films were generally lower than the CD films except for the LBL films prepared at rf powers of 20 and 40 W. This indicates that the LBL films are generally more ordered compared to the CD films. Hydrogen plasma treatment in LBL processes plays an important role in enhancing the structural order of the films by reducing the disprder from grain boundaries.

Figure 4.15(a) showed the R^* for the CD films increased linearly with increase in rf power. This is consistent with results obtained from similar studies on continuously deposited nc-Si:H thin fims by rf-PECVD. The increase in disorder of the silicon matrix is due to increase in the surface temperature as a result of high ion bombardment effect on the film surface (Chowdhury *et al.*, 2007). However, the R^* for the LBL films showed a different trend as compared to the CD films. For these films, the R^* decreased gradually from 0.45 to a slightly lower value around 0.3 with increase in rf power from 20 to 60 W and increased slightly to around 0.4 with further increase in rf power to 100 W. This revealed that the LBL films were most ordered comparatively when prepared at rf powers between 40 to 60 W. The films prepared at 20 W and the high rf powers of 80 and 100 W had high concentration of dihydrides either in the grain boundaries surrounding the Si nano-crystallites or in the amorphous matrix. At the low rf power of

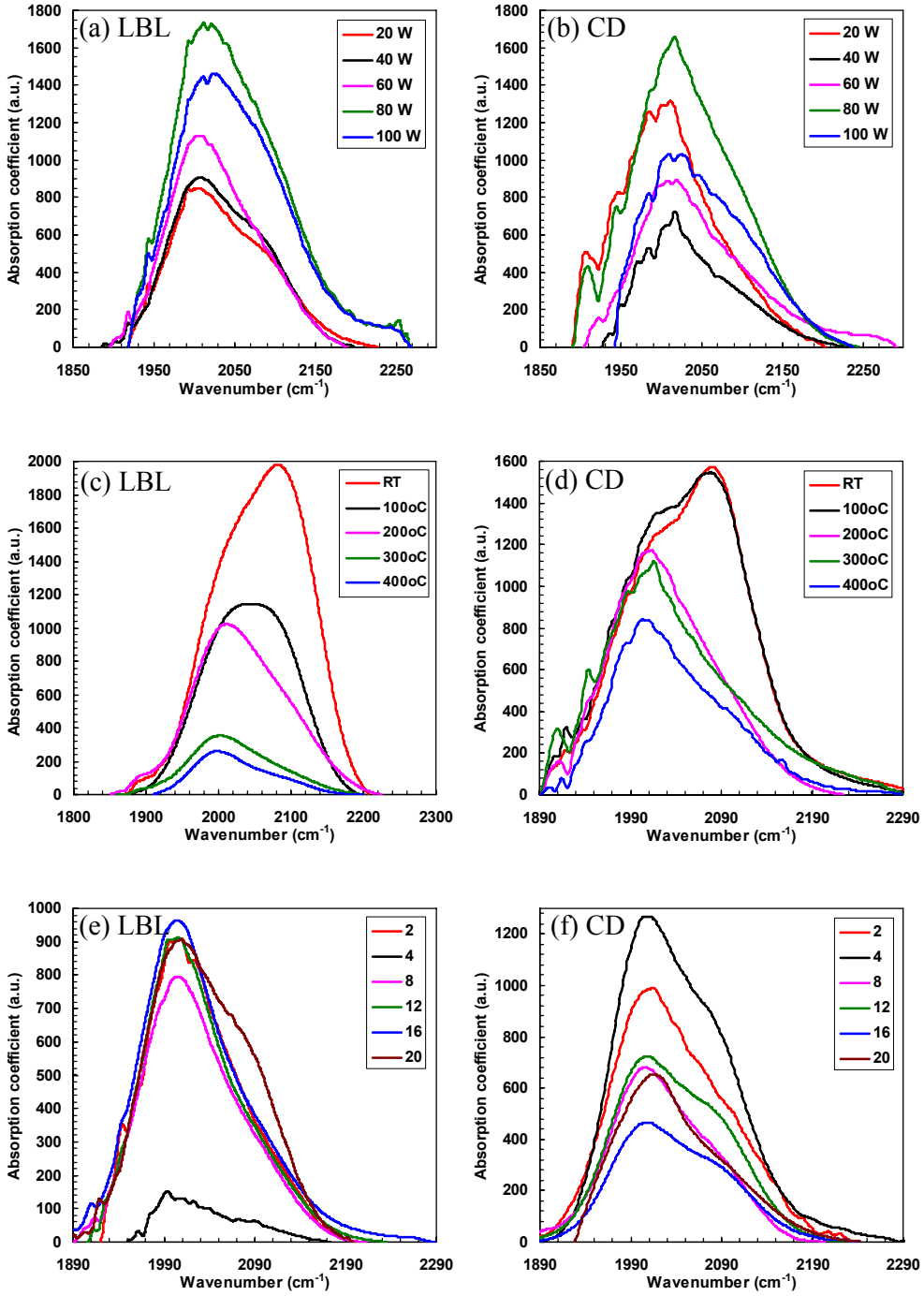

Figure 4.14: Absorption coefficient at 1850 – 2250 cm^{-1} for the LBL and CD films deposited at various rf powers (a) and (b), substrate temperatures, T_s (c) and (d) and hydrogen to silane flow-rate ratio, R (e) and (f).

20 W, the hydrogen etching effect of the hydrogen plasma treatment was probably low thus increasing the disorder in the film structure. At the high rf powers, the enhancement in the hydrogen etching effects may form Si nano-crystallites with large grain boundaries thus enhancing the R^*. Increase in ion bombardment effects at high rf powers may also contribute to the increase in disorder of the films as in the CD films. The films prepared at rf powers between 40 to 60 W were most ordered as the hydrogen etching effects may have formed Si nano-crystallites with low volume fraction of grain boundaries and the bombardment effects was not destructive enough to result in disorder in the film structure. This agrees with reports that low crystalline volume fraction as a result of formation of high density of grain boundaries of dihydrides $Si\text{-}H_2$ or polyhydrides $(Si\text{-}H_2)_n$ surrounding the Si nano-crystallites can increase the disorder in nc-Si film structure.

It is interesting to note that the R^* for the LBL and CD films showed similar trends with T_s as shown in Figure 4.15(b). The R^* decreased gradually to a low saturation value for the films prepared at T_s of 200°C. The values of R^* for LBL films were significantly lower compared to the CD films. This clearly showed increase in substrate temperature increased the structural order in the film structure irrespective of the deposition techniques but hydrogen etching effect during the hydrogen plasma treatment of the LBL processes was more effective in reducing the structural disorder in the films.

Figure 4.15(c) showed that increase in the hydrogen to silane flow-rate ratio, R increased the structural order in the film structure for both LBL and CD films. Again, all the values of the R^* for the LBL films were lower than the CD films at all R. This again showed that hydrogen etching effect in the LBL processes improve the structural order in the film structure. Increase in R produced more atomic hydrogen reaching the growing surface thus enhancing the hydrogen etching effect and therefore result in an

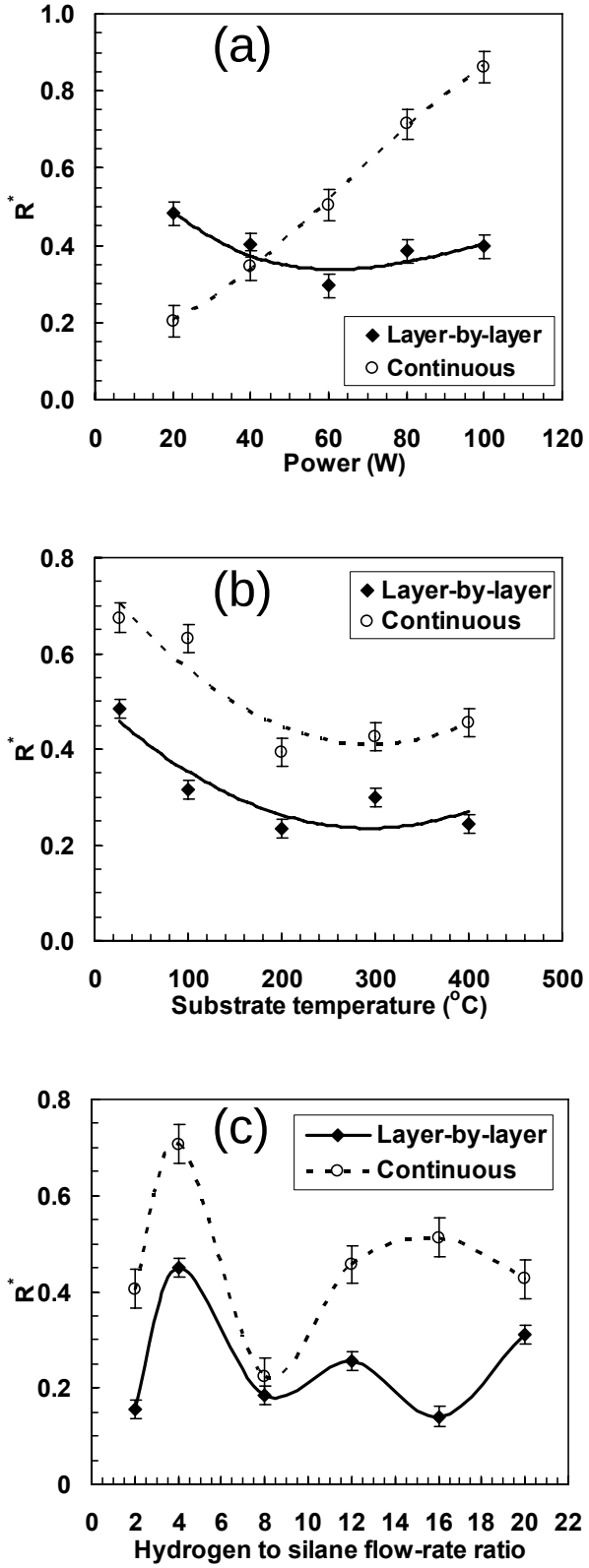

Figure 4.15: Variation of R^* of the films with (a) rf power, (b) substrate temperature, T_s and (c) hydrogen to silane flow-rate ratio, R.

increase in the structural disorder in the film structure. This could also be due to the formation of Si nano-crystallites with significant volume fraction of grain boundaries of Si-H_2 bonds as hydrogen etching effects are reported to be effective in the formation of Si nano-crystallites. The increase in the presence of H atoms contributed to the formation the grains surrounding these nanocrystallites.

4.5 X-Ray Diffraction (XRD) Spectra

The X-ray diffraction (XRD) is a useful characterization technique that provide structure orientation of the crystalline sample and crystallinity of biphasic thin film such as Si:H thin film. In this work, the XRD spectra were used to study the crystallinity of mixed phases of Si:H thin films consisting of nanocrystallites embedded within an amorphous matrix (Guha *et al.*, 1999). These XRD spectra were obtained using a SIEMENS D5000 diffractometer with thin film attachment operating with CuK_α radiation. The scanning range is set at 20 to 80 ^{o} with step size and step time of 0.02 ^{o} and 3 s respectively. Usually, the crystalline silicon showed diffraction peaks at diffraction angle of 28.4, 47.3 and 56.1 ^{o} which correspond to c-Si orientations of (111), (220) and (311) respectively (Mahan, 2000). Figure 4.16 shows a typical XRD spectrum of Si:H thin film deposited by PECVD technique consisting of mixed phases of amorphous and crystalline Si structure. The appearance of broad peak at about 14^o is an indication of amorphous phase in the film. A typical XRD spectrum of c-Si substrate is shown in the inset of the figure. Also, a typical XRD spectrum of glass substrate is shown in Figure 4.17.

Figure 4.18 presents the XRD spectra for the LBL and CD films deposited on c-Si (111) and glass substrates at different rf powers. For the films on c-Si in Figure 4.18(a) and (b), both the LBL and CD films showed crystalline diffraction peaks at 2θ angle around 28 and 56 ^{o} indicating preferred crystalline orientation planes are the Si

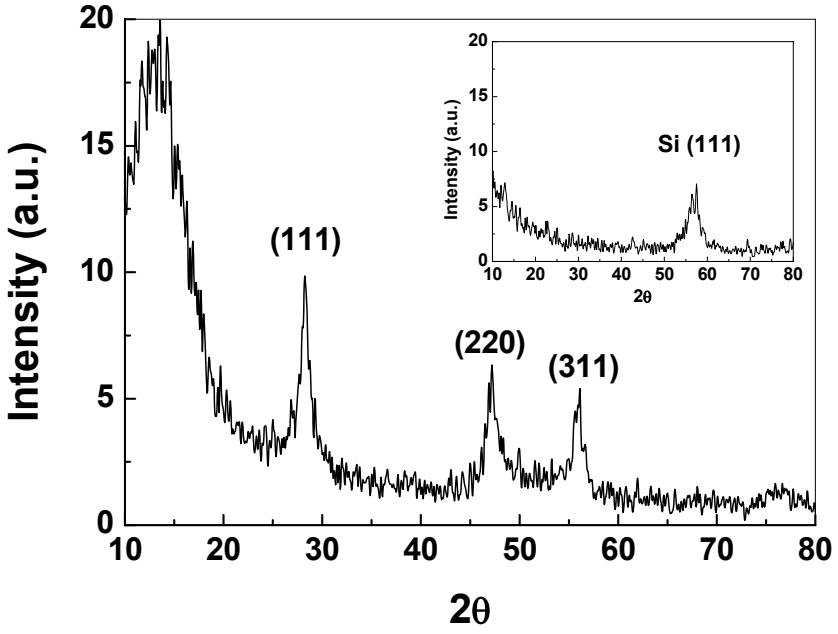

Figure 4.16: Typical XRD spectrum of mixed phases of Si:H thin film deposited by rf-PECVD technique. Typical XRD spectrum of c-Si substrate is shown in the inset.

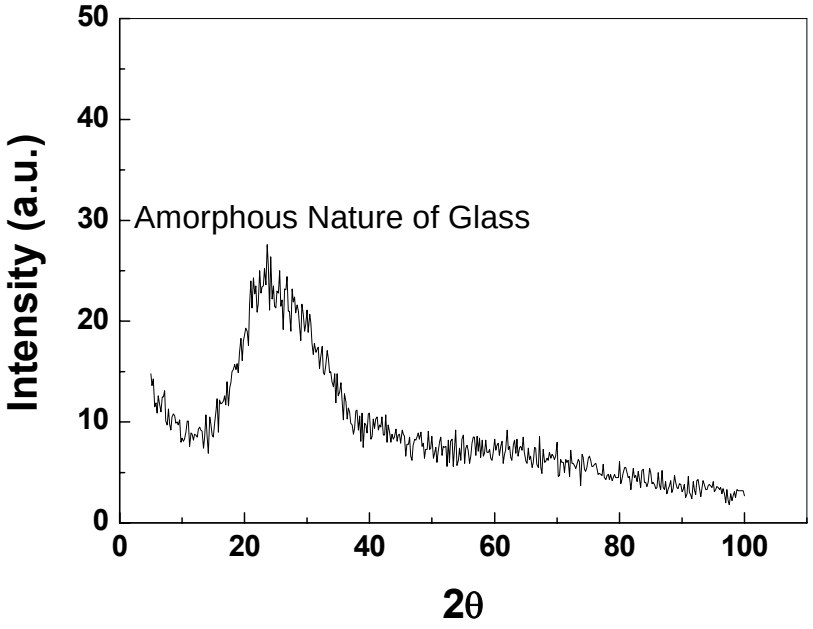

Figure 4.17: Typical XRD spectrum of glass substrate.

(111) and Si (311) respectively. The LBL films consistently showed sharp crystalline peaks at 56°C which increased in intensity with increase in rf power. As for the CD film only the film prepared at rf power of 20 W produced a relatively sharp peak at this 2θ angle. The XRD spectra of a bare c-Si (111) used as the substrate for these films also shows a sharp peak at 2θ angle of 56^{o} and it is natural to believe that this peak is contributed by the substrates. However, if this is so, the peak intensity is expected to increase with decrease in film thickness. Referring to Figure 4.3, the deposition rate is proportional to the film thickness since the films were deposited at fixed time duration. Therefore, the order of film thickness from the thickest to the thinnest film are LBL (20W), LBL (40W), LBL (60W), LBL (80W), LBL (100W), CD (100 W), CD (80 W), CD (60W), CD (40W) and CD (20W). The thickness of the LBL (60W), LBL (80W), LBL (100W), CD (100 W), CD (80 W) and CD (60W) are approximately the same and therefore the crystalline peaks should be of the same order of sharpness. The CD (40W) and CD (20W) films should have the sharpest peaks compared to the other films in the Si (311) orientation planes but obviously these are not the case for these films. The results therefore indicated that the c-Si (111) lattice structure acted as seeding layer for nanocrystalline growth at the preferential of Si (311) orientation plane and hydrogen plasma treatment process for the LBL films enhanced the crystallinity of the films. Also increase in rf power induced further enhancement in nanocrystalline growth in the LBL films. The lattice structure of the c-Si substrate becomes the template for the formation of crystalline structures in the film. With increase in film thickness, the effect of this lattice as template is reduces thus resulting in decrease in the crystalline structure in the film as discussed above. The degree of crystallinity shown by the Si (111) plane however showed no dependence on rf power for the LBL films. The Si (311) peak decreased in sharpness with increase in rf power for the CD films but the Si (111) peak on the other hand appeared to increase in sharpness with increase in rf power. Increase

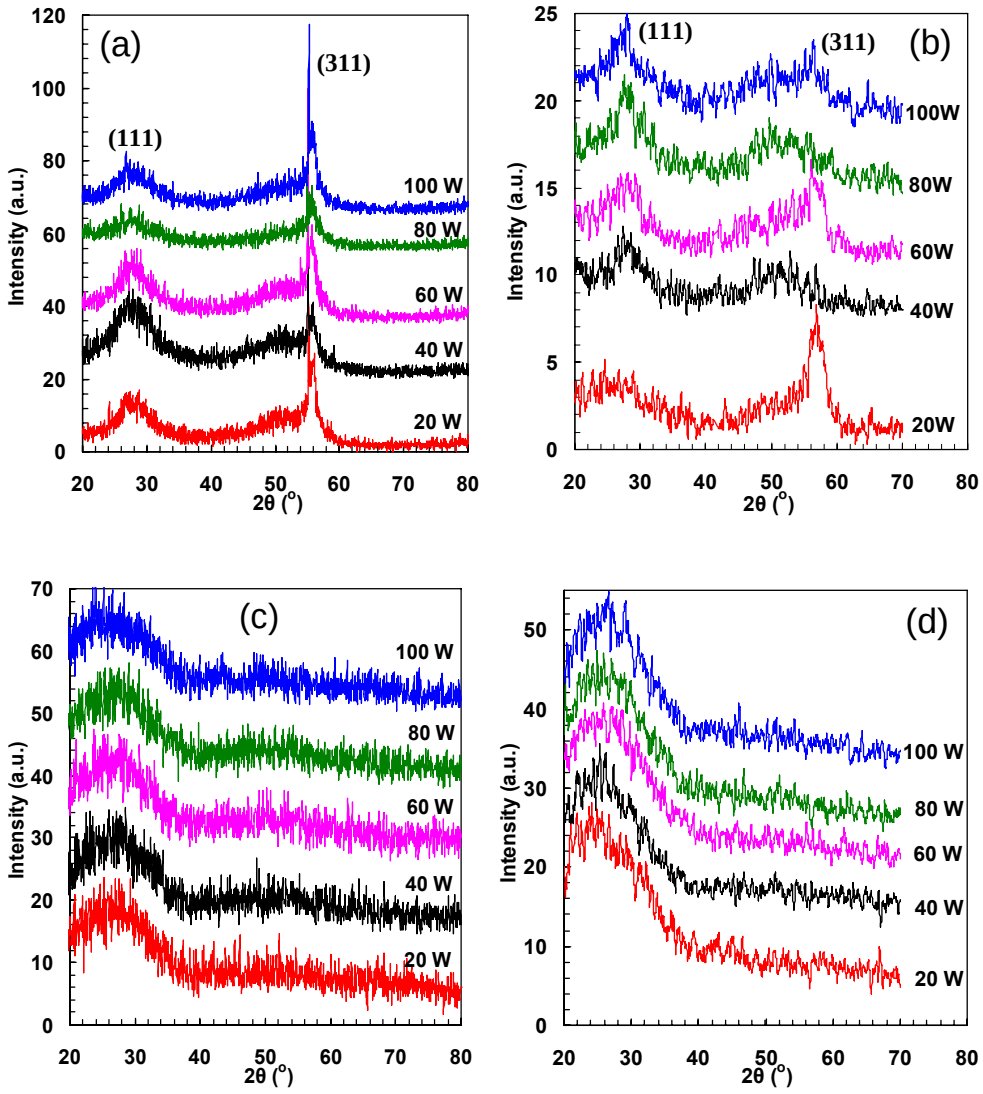

Figure 4.18: XRD of (a) LBL and (b) CD films deposited on c-Si (111) substrates, and (c) LBL and (d) CD films deposited on glass substrates, prepared at different rf powers.

in rf power produced a change in the preferred orientation plane from Si (311) to Si (111) with increase in rf power. The increase in structural disorder of the CD film structure with increase in rf power as indicated by increase in microstructure parameter, R^* as shown in Figure 4.15(a) was said to be contributed by the increase in ion bombardment on the growth surface with increase in rf power. Thus, the change in the preferred orientation planes of the Si nano-crystallites in the CD films from Si (311) to Si (111) orientation plane induced enhancement in the structural disorder in the film structure. The ion bombardments effects may have induced the transformation of the

preferred orientation planes of the Si nano-crystallites from the Si (311) plane to Si (111) plane. Figure 4.18(c) and (d) showed that the XRD spectra of Si:H films prepared on glass substrates produced broad diffraction peaks at 2θ angle around 28^{o} indicating that the films were generally amorphous with sparsely scattered Si nano-crystallites. This shows that formation of Si nano-crystallites in films were substrate dependent. The c-Si (111) substrate may act as a seeding layer for the formation of the crystalline Si nanostructures and periodic hydrogen plasma treatment on the growth surface enhanced the formation of the Si nano-crystallites especially when deposited at high rf power. In continuous deposition, increase in rf power suppressed the crystallinity in the Si (311) orientation plane but increased the crystallinity in the Si (111) orientation plane.

Figure 4.19 presents the XRD spectra for the LBL and CD films deposited on c-Si (111) and glass substrates different T_s. These results again confirmed that c-Si (111) substrate acted as a seeding layer inducing the formation of nc-Si structures and the LBL deposition enhanced the formation of these nanocrystallites from the higher intensity and sharper peaks in the XRD spectra of the films indicating preferred orientation at the Si (311) plane. Increased surface mobility and diffusion of hydrogen atoms at higher substrate temperatures up to 300°C enhanced the crystallinity of the films. The hydrogen plasma treatment for the LBL processed films even showed formation of Si nano-crystallite in the films prepared at room temperature and increase in substrate temperature up to 300°C increased the crystallity in the films. For the CD films, increase in crystallinity was only observed in the films deposited at 200 and 300°C. The crystallinity decreased in the films prepared at 400°C for both the CD and LBL films. The lower bonded hydrogen content in the film may contribute to the lower crystallinity of the films prepared at this high temperature possibility due to the presence of high concentration of dangling bonds. Increasing substrate temperature was seen to be ineffective in increasing the crystallinity in both the LBL and CD films

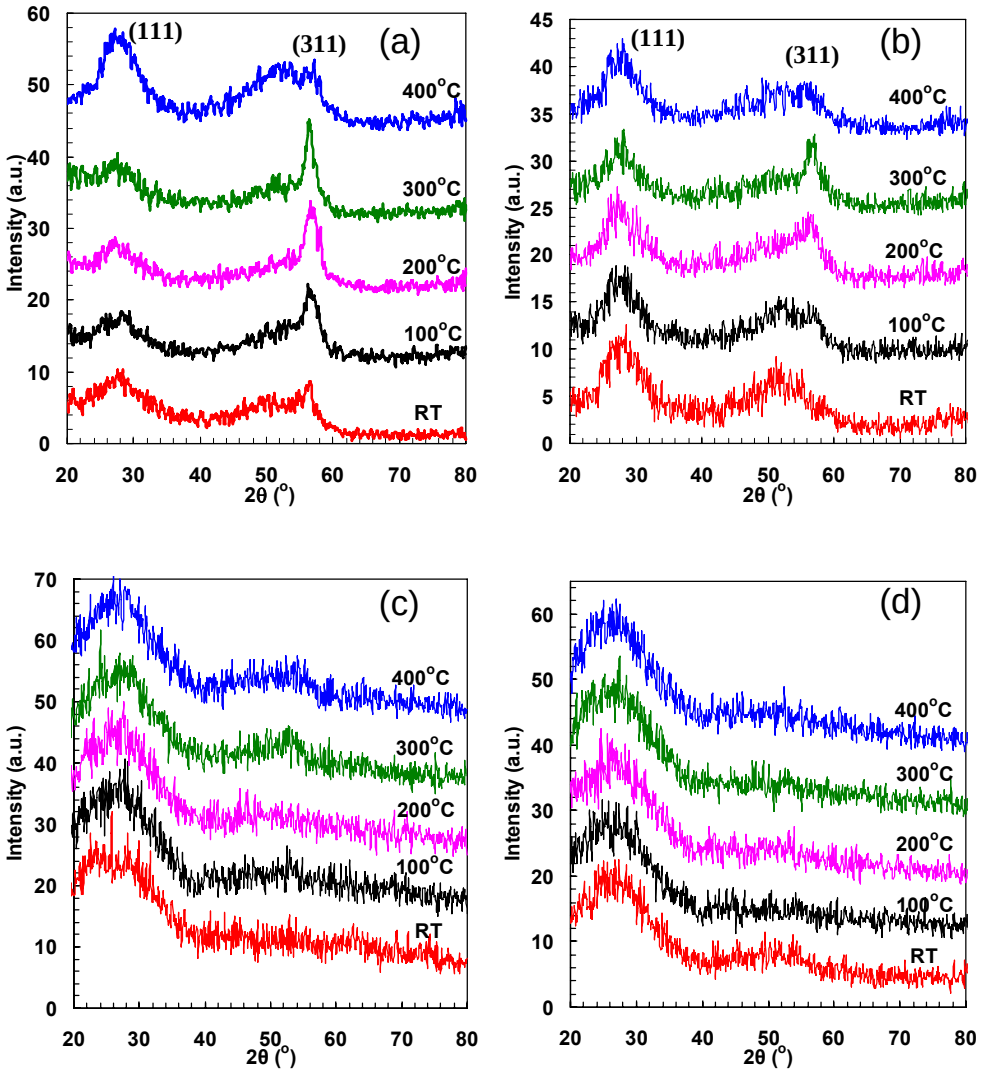

Figure 4.19: XRD of (a) LBL and (b) CD films deposited on c-Si (111) substrates, and (c) LBL and (d) CD films deposited on glass substrates, prepared at different substrate temperatures, T_s.

deposited on glass substrates. Insignificant presence of sparsely distributed nanocrystalline grains produced broad diffraction peak at 2θ around 28 ° corresponding to the Si (111) orientation plane.

Figure 4.20 shows the XRD spectra of LBL and CD films deposited on c-Si (111) and glass substrates at different *R*. Both the LBL and CD films deposited on c-Si showed highest crystallinity with preferred orientation in the Si (311) plane for the films prepared at *R* equals to 12. This indicated again that the lattice of c-Si (111) substrate acted as a seeding layer for preferred Si (311) orientation nanocrystalline growth.

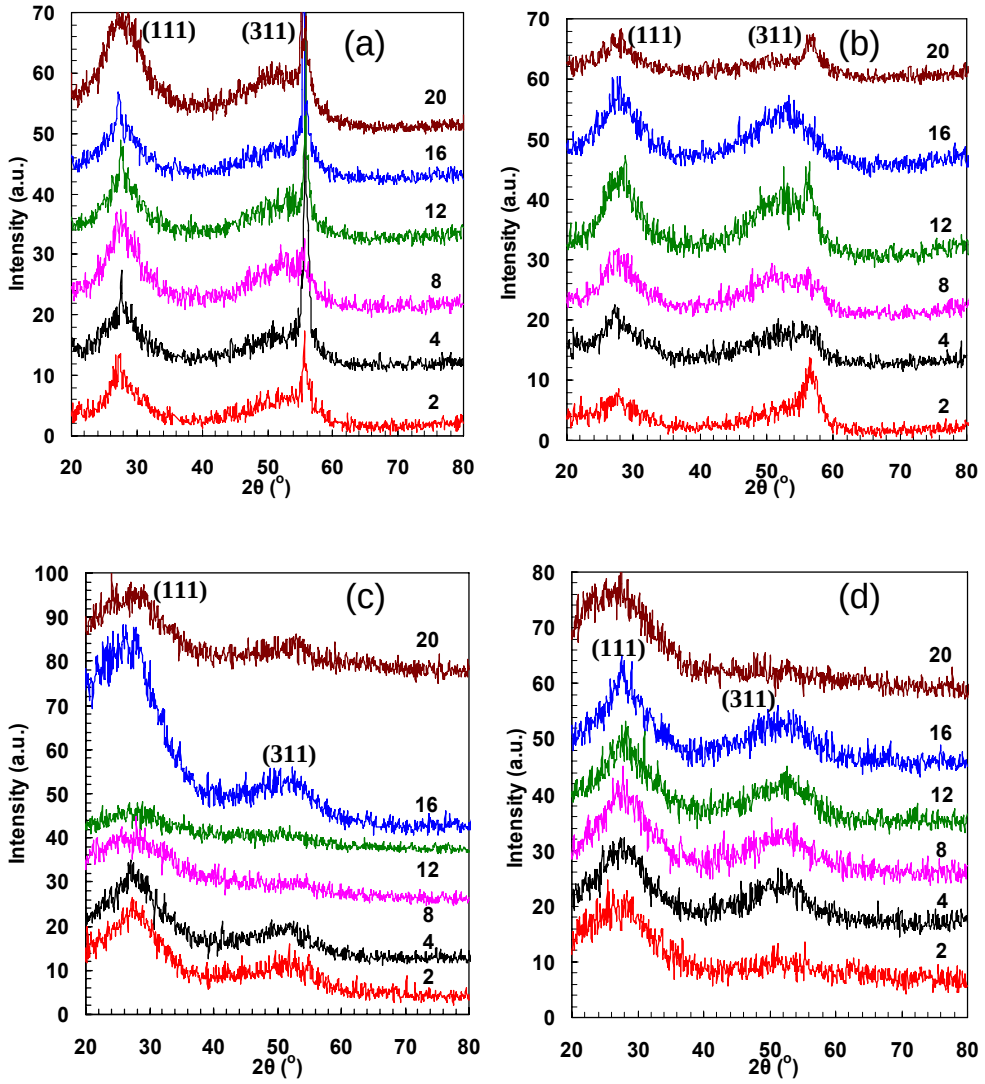

Figure 4.20: XRD of (a) LBL and (b) CD films deposited on c-Si (111) substrates, and (c) LBL and (d) CD films deposited on glass substrates, prepared at different hydrogen to silane flow-rate ratios, *R*.

However, the consistency in the results for both LBL and CD deposited films on this substrate showed that the concentration of SiH_3 growth radicals and energy of hydrogen atoms reaching the growth surface during the growth process had significant influence on the formation of nc-Si. The energy of the hydrogen atoms determined the effectiveness of the hydrogen etching process in creating nucleation sites for diffusion of the radicals and the concentration of growth radicals at the growth surface must be sufficient to diffuse into the nucleation sites created otherwise the films would be high

in hydrogen content. Therefore, R of 12 produced the optimized SiH_x (x = 1,2,3) radicals through dissociation of silane and hydrogen molecules to promote secondary reactions to produce the highest concentration of SiH_3 radicals and hydrogen atoms with the highest energy for the formation of Si nano-crystallites. Low R resulted lower number hydrogen atoms reaching the growth sites thus reducing hydrogen etching effects and high R reduced the number of SiH_3 radicals reaching the growth sites as hydrogen dilution was high and the energy of of the hydrogen atoms were low due to increase in frequency of collisions with undissociated molecules. However, the higher crystallinity of the LBL film prepared at this R showed that the periodic hydrogen plasma treatment of the growth surface induced higher crystallinity in the films. Again, crystallinity for both the LBL and CD films deposited at all R was very low for the films deposited on glass substrates.

4.6 Summary

The results on the effects of rf power, substrate temperature and hydrogen to silane flow-rate ratio on the optical and structural properties of the LBL and CD films deposited Si:H films have been presented and discussed in this chapter.

In the LBL process, nucleation of the growth sites was mainly induced during the hydrogen plasma treatment process while in the CD process, growth and nucleation occurred simultaneously throughout the deposition process. This produced the reversed trends in growth rates for LBL and CD films with respect to rf power and substrate temperature. The deposition rate of the LBL films decreased with increase in rf power and vice-versa for the CD films. Similarly, the deposition rate of the CD films showed a reversed trend with substrate temperature compared to the LBL film. The deposition rate of the LBL films increased with increase substrate temperature and vice-versa for the CD films. The hydrogen to silane flow-rate ratio showed strong capability of

enhancing the growth rates both for CD and LBL films. The growth rates of the CD films and LBL films reached a maximum at different gas flow-rate ratio. The LBL process produced lower maximum growth rate at lower gas flow-rate ratio compared to CD films.

The optical transmission spectra of the films showed that substrate temperature has significant influence on the change in the phase structure of both LBL and CD films deposited on glass substrates. However, the XRD spectra of the films on glass substrates showed that the films were amorphous structure irrespective of the rf power and substrate temperature. The compactness of the film structure was shown to be strongly influenced by the deposition conditions such as rf power and substrate temperature. LBL films prepared at low rf power of 40 W and substrate temperature of 300^{o}C had the highest refractive index indicating a highly compact film structure.

Substrate temperature has strong influence on optical energy gap in LBL films. The optical energy gap decreased significantly from 1.85 to 1.65 eV with increase in substrate temperature from 100 to 400^{o}C. Substrate temperature in this range has shown to be very effective in tuning the band gap of the LBL deposited films. The LBL deposited films prepared on c-Si substrates showed that the hydrogen content produced similar trend with respect to substrate temperature as optical energy gap with respect to substrate temperature. This strongly showed that optical energy gap has strong dependence on the hydrogen content in the films and the hydrogen content in the films prepared on c-Si and glass substrates have similar dependence on substrate temperature.

The trend of oxygen contamination appeared to be reversed with respect to the LBL films as high substrate temperature increased oxygen contamination in the CD films. Hydrogen plasma treatment in the LBL process at high substrate temperature appeared to be very effective in reducing oxygen contamination in the film structure. LBL deposited films were more ordered compared to the CD films. The hydrogen

etching effect during the hydrogen plasma treatment of the LBL processes was shown to be effective in reducing the structural disorder in the films especially with increase in substrate temperature.

The c-Si (111) substrate was seen to act as a seeding layer for the formation of the crystalline Si nanostructures and the periodic hydrogen plasma treatment on the growth surface enhanced the formation of the Si nano-crystallites especially when deposited at high rf power. The films prepared by LBL deposition process were more crystalline than the CD films and the films deposited on c-Si substrates also showed significantly higher crystallinity compared to the films grown on glass substrates. Substrate temperature and rf power were shown to have significant influence on the crytallinity of the Si:H films particularly for the LBL films deposited on c-Si substrates.